W Boson Mass Measurement Using CDF-II Detector

Guillelmo Gómez-Ceballos

Massachusetts Institute of Technology

Milano-Bicocca Seminar, June 2022

Motivation for Precision Measurements

- Electroweak gauge sector of the standard model (SM) is constrained by precisely known parameters
  - $\alpha_{EW}(m_{\mathrm{Z}}) = 1/127.918(18)$
  - $G_F = 1.16637(1) \times 10^{-5}\ \mathrm{GeV}^{-2}$
  - $m_{\mathrm{Z}} = 91.1876(21)\ \mathrm{GeV}$
  - $m_{top} = 172.89(59)\ \mathrm{GeV}$
  - $m_{\mathrm{H}} = 125.25(17)\ \mathrm{GeV}$
- At tree-level, these parameters are related to m_{W}
  - $m_{\mathrm{W}}^2 = \frac{\pi \alpha_{EW}}{\sqrt{2} G_F sin^2\theta_{\mathrm{W}}}$
  - $sin^2\theta_{\mathrm{W}} = 1 - m_{\mathrm{W}}^2/m_{\mathrm{Z}}^2$
- Radiative corrections due to heavy quark and Higgs loops and (potentially) undiscovered particles
  - $m_{\mathrm{W}}^2 = \frac{\pi \alpha_{EW}}{\sqrt{2} G_F sin^2\theta_{\mathrm{W}}}(1 + \Delta r)$
  - $\Delta r = f(m_{top}^2, \ln(m_{\mathrm{H}}), ...)$
- m_{top}, m_{H}, and m_{W} tightly constrained within SM:
  - SM expectation $m_{\mathrm{W}} = 80357 \pm 4_{\mathrm{inputs}} \pm 4_{\mathrm{theory}}\ \mathrm{MeV}$

m_{W} vs. m_{top} (Before New CDF Measurement)

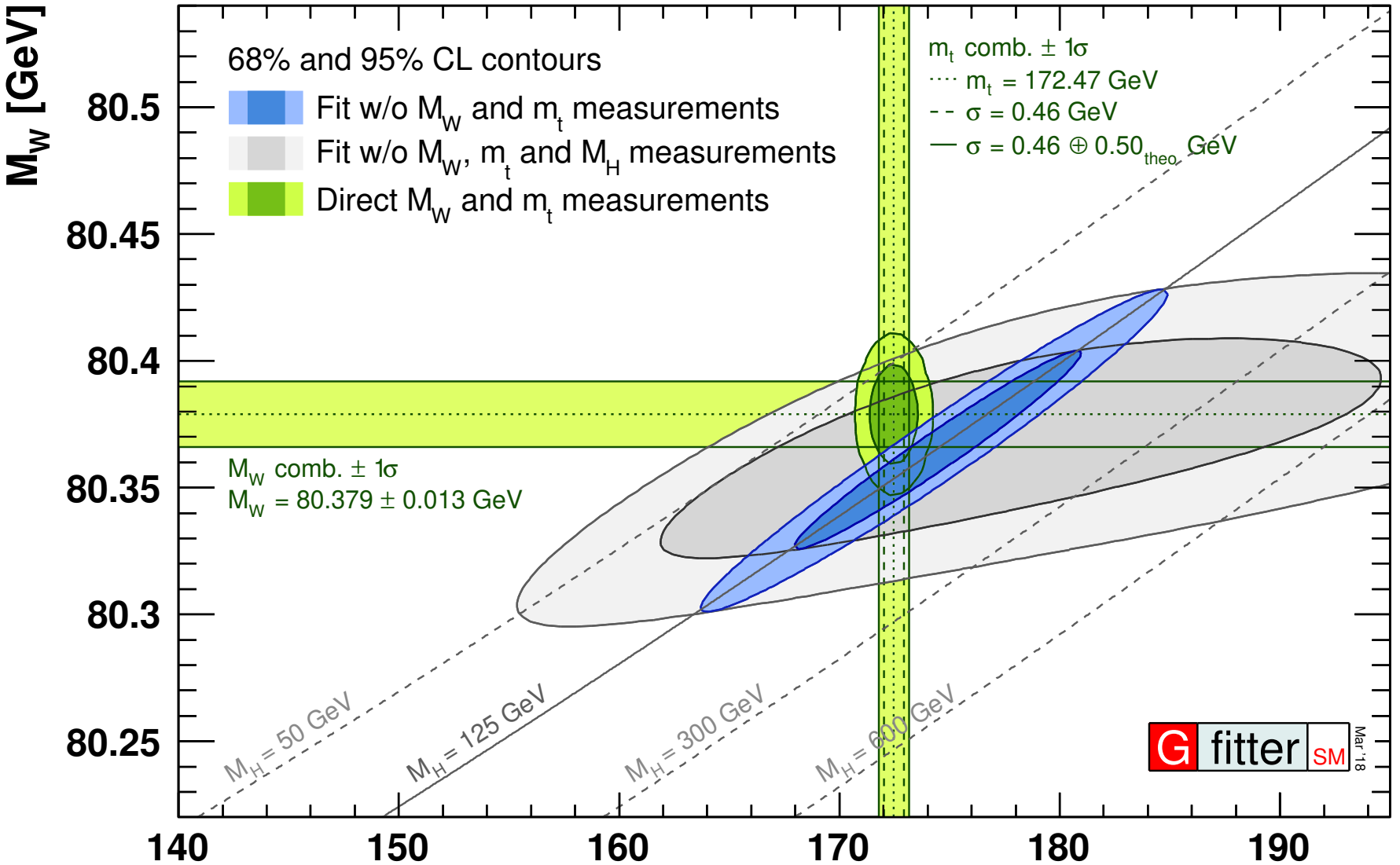

Need high precision to be sensitive to non-SM physics

A m_{W} measurement is also an incredible milestone for an experiment

Colliders: A Reminder

- LEP: $\mathrm{e^+e^-}$ collider
  - LEP-I: $\sqrt{s} \sim m_{\mathrm{Z}}$, high precision measurements, still unbeatable today
  - LEP-II: $\sqrt{s} \sim 130 - 209\ \mathrm{GeV}$, W physics, Higgs searches, limits on exotic models till its kinematical threshold
  - total integrated luminosity: $\sim 1\ \mathrm{fb}^{-1}$
  - very clean environment
- Tevatron: $\mathrm{p\bar{p}}$ collider
  - CDF-I: $\sqrt{s} \sim 1.8\ \mathrm{TeV}$, CDF-II: $\sqrt{s} \sim 1.96\ \mathrm{TeV}$
  - top and B-physics (observation of top-quark, B_s mixing oscillations...)
  - total integrated luminosity: $\sim 10\ \mathrm{fb}^{-1}$
  - 2–3 additional $\mathrm{p\bar{p}}$ interactions in the same and nearby bunch crossings (pileup)
- LHC: pp collider
  - Run 1: $7 - 8\ \mathrm{TeV}$, $\sim 25\ \mathrm{fb}^{-1}$, Higgs boson observation
  - Run 2: $13\ \mathrm{TeV}$, $\sim 140\ \mathrm{fb}^{-1}$, differential measurements, observation of rare processes
  - 20-50 pileup events, major drawback of LHC w.r.t. Tevatron!

Measuring W Boson Mass

- e^+e^- colliders
  - direct mass measurement using $WW \to qqqq/qq\ell\nu$ events
    - energy and momentum conservation allows for very precise measurements
    - missing momentum from neutrinos can also be known
  - energy scan around $\sim 2 \times m_W$
    - very strong σ_{WW} dependence of m_W close to energy kinematic threshold
- Hadron colliders
  - only $W \to \ell\nu$ decays can be realistically speaking be used
  - only missing transverse momentum (p_T^{miss}) can be inferred, longitudinal component unknown
  - a set of variables can be used to indirectly measuring m_W:
    - p_T^ℓ
    - p_T^{miss}
    - $m_T = \sqrt{2 p_T^{miss} p_T^\ell cos(1 - \Delta\phi(p_T^{miss}, p_T^\ell))}$

e^+e^- Colliders

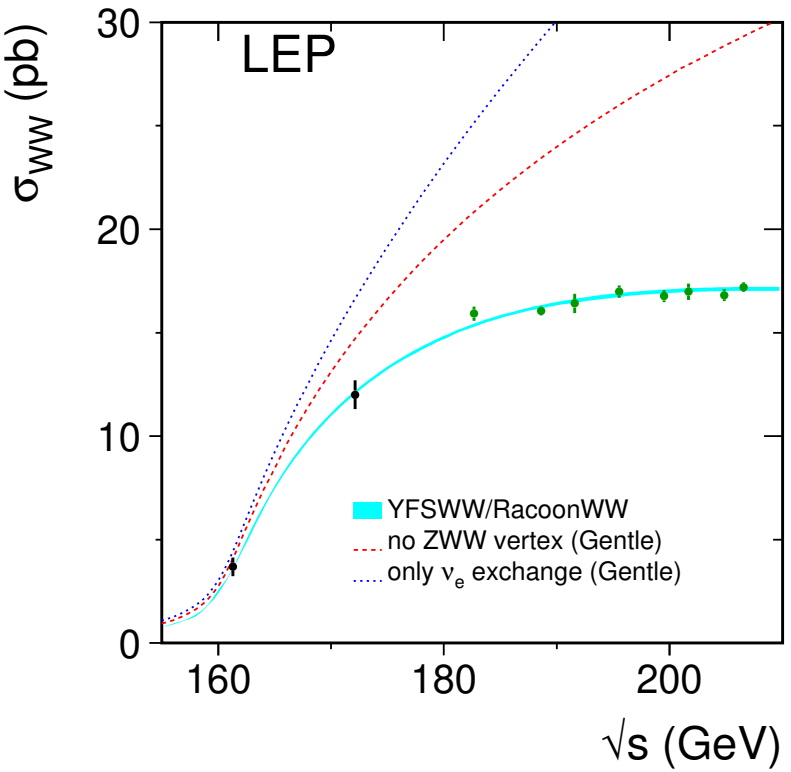

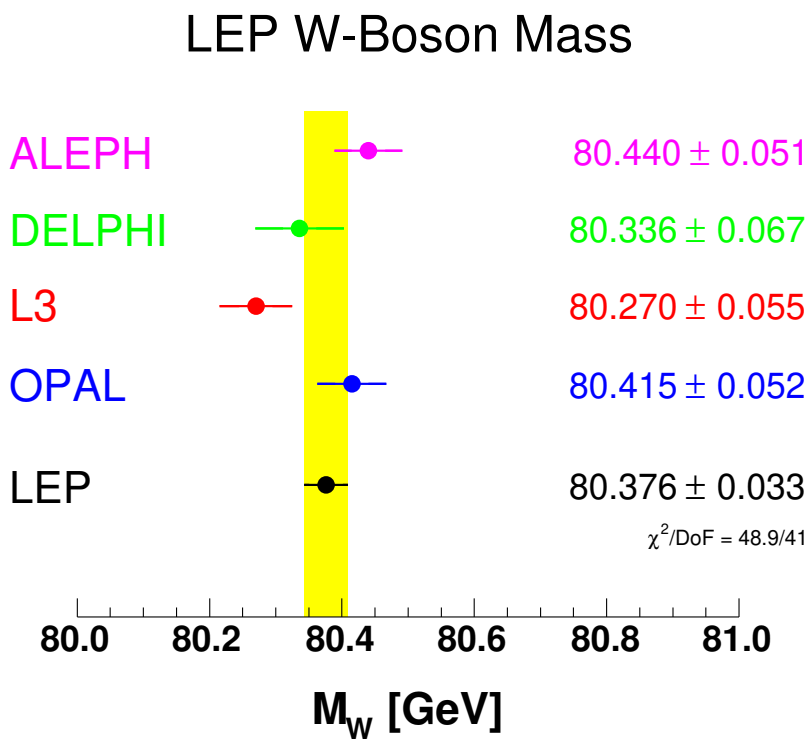

- $m_{\mathrm{W}}(\text{threshold}) = 80420 \pm 200(\text{syst.}) \pm 30(\text{LEP energy})\ \mathrm{MeV}$
- $m_{\mathrm{W}}(\text{direct}) = 80375 \pm 25(\text{stat.}) \pm 22(\text{syst.})\ \mathrm{MeV}$
- With larger data sets (FCCee, ILC...), e^+e^- collisions would reach the "ultimate" precision

Example: τ Mass Measurements

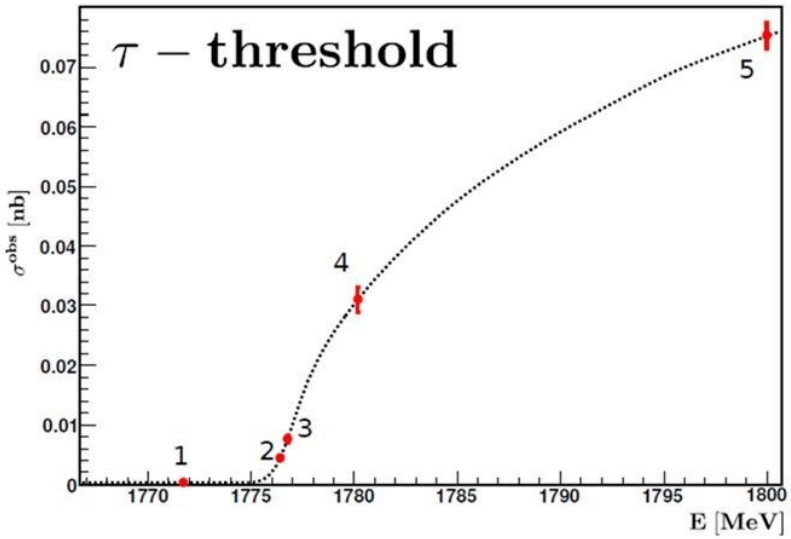

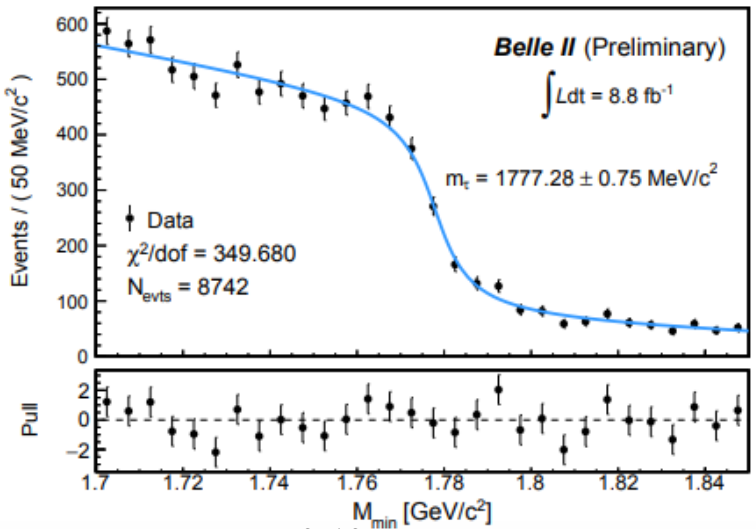

- m_τ (BES, energy scan) $= 1776.91 \pm 0.12(\text{stat.})^{+0.10}_{-0.13}(\text{syst.})$ MeV
- m_τ (BELLE, pseudo-mass) $= 1777.28 \pm 0.75(\text{stat.}) \pm 0.33(\text{syst.})$ MeV
  - $M_{min} = \sqrt{m_{3\pi}^2 + 2(E_{beam} - E_{3\pi})(E_{3\pi} - P_{3\pi})} \leq m_\tau$

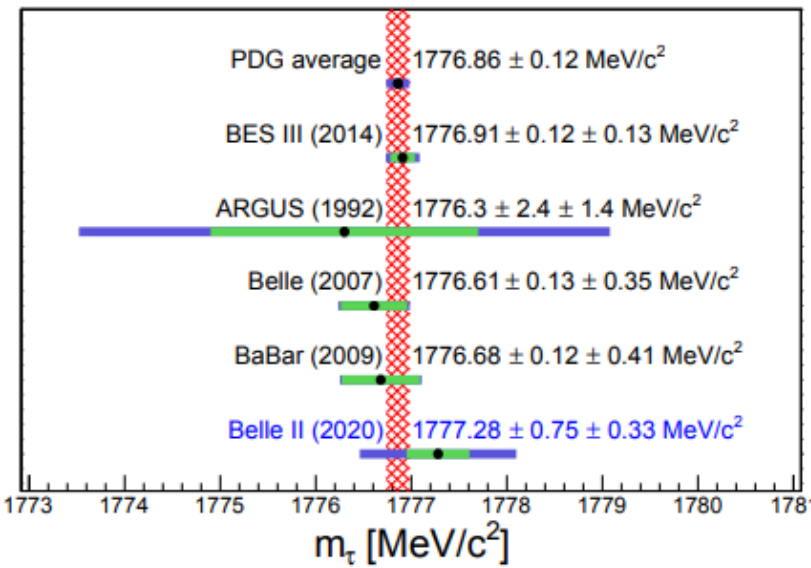

Hadron Colliders

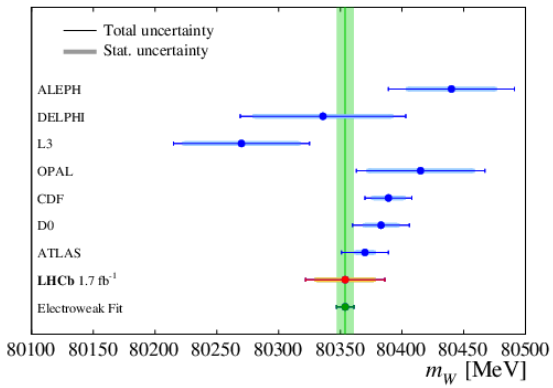

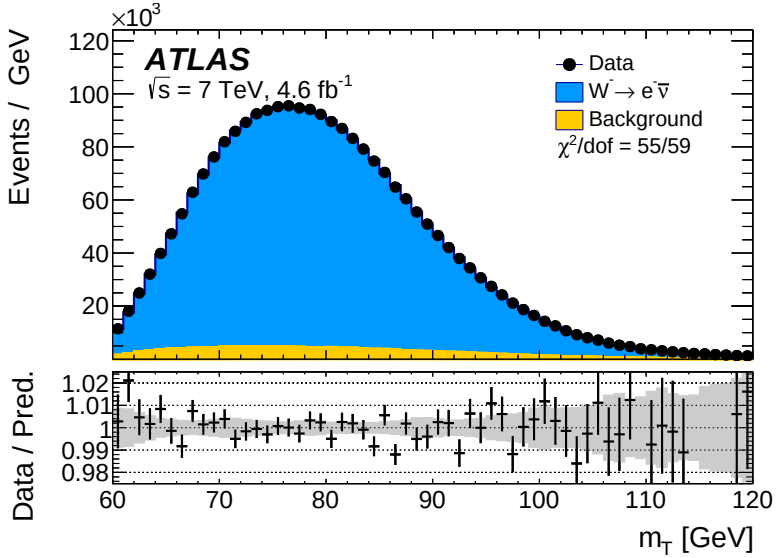

- Analyses largely systematic limited
- Theoretical uncertainties play a keep role since cannot directly access m_{W}
- Fit measurements will become more and more complicated to overcome this limited theoretical knowledge

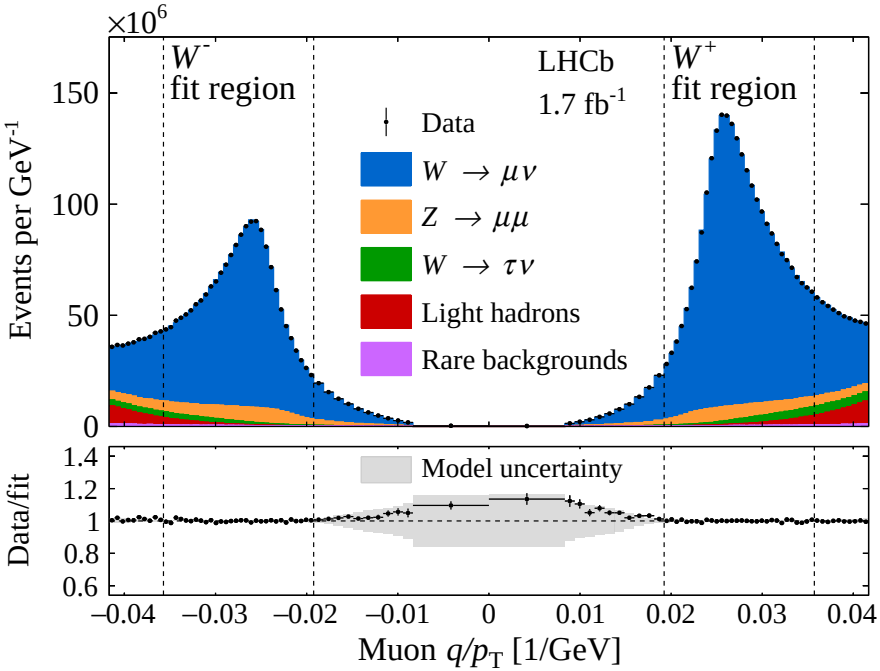

Tevatron vs. LHC for A W Boson Mass Measurement

- Much harder data taking conditions at LHC due to $\sim$10 times more pileup events (although not on the current public analyses)
- Tevatron, $\mathrm{p\bar{p}}$ collider, running at lower $\sqrt{s}$ values imply quark-dominated interactions, much lower parton distribution functions (PDFs) and theoretical uncertainties upfront
- Much lower integrated luminosity per year at the Tevatron due to the lower pileup (effect is $\sim$ linear), but also due to the more difficulty to produce antiprotons
- For the same integrated luminosity, the number of W boson events is about 10 times larger at LHC
  - a factor of $\sim$ 5 larger cross sections
  - a factor of $\sim$ 2 larger detector coverage
- LHC analyses become systematic limited much quicker
- Running at low pileup for a long(er) time at LHC?
  - would be the best choice, but it comes to a price of lower integrated luminosity for the same running time
  - LHC was built to find rare processes, which require large data sets, to the cost of much harder data taking conditions

W & Z Boson Production at CDF

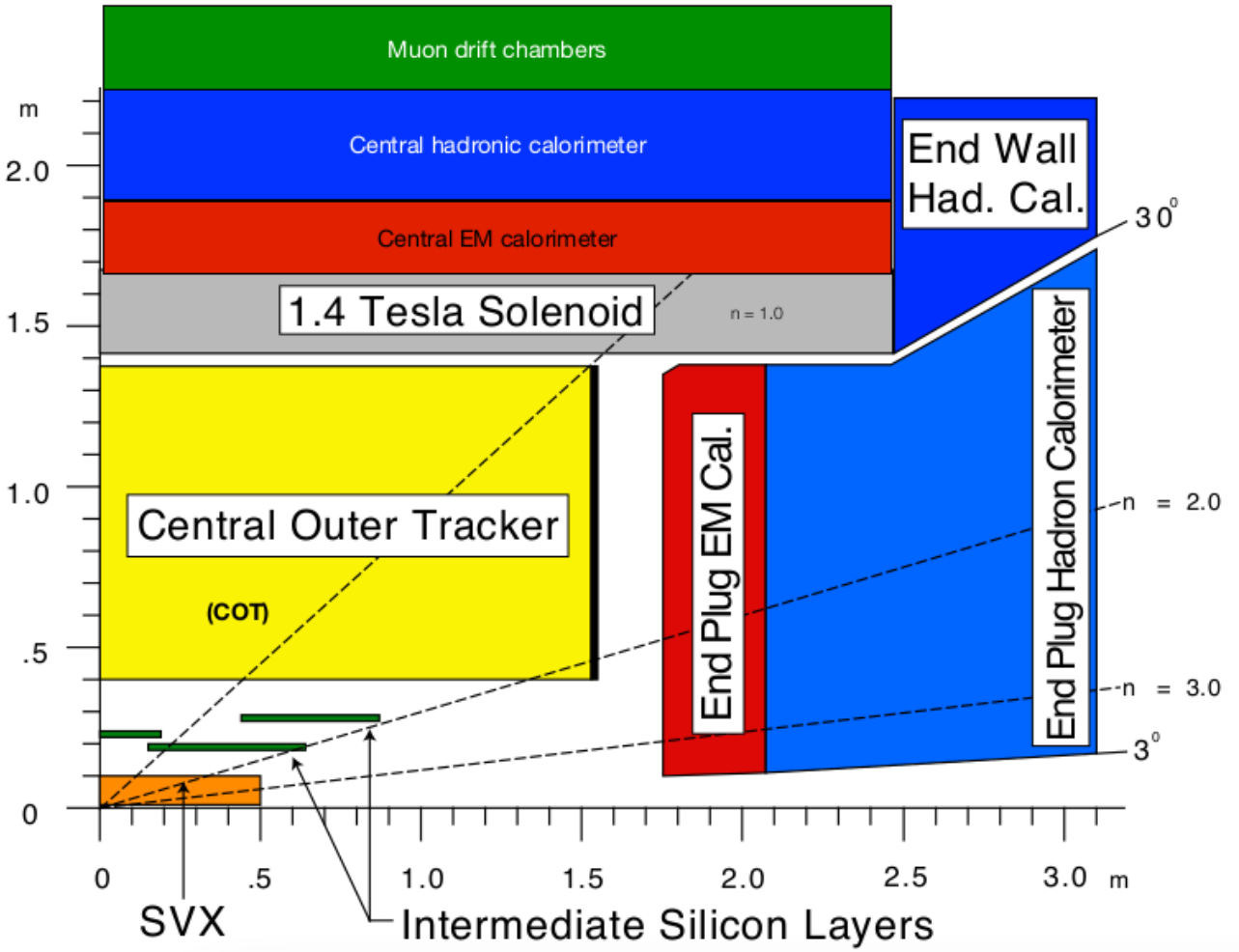

- $\mathrm{W} \to \ell\nu$ and $\mathrm{Z} \to \ell\ell$ events ($\ell = \mathrm{e}, \mu$) with charged leptons within $|\eta| < 1$
- This ensures full central tracker (COT), central calorimeter (CEM), and muon chambers (CMX) coverage

Analysis Strategy in a Glance

- Selection, signal, & backgrounds
  - event selection & background estimation
  - simulation & template fitting
- Theoretical treatment
- Calibration measurements
  - muon momentum calibration
  - electron momentum calibration
  - recoil calibration & validation
    - hadronic recoil $|\vec{u}| = |\sum_i E_i sin\theta_i|$, $|\vec{u}| \simeq p_{\mathrm{T}}^{\mathrm{W}}$
    - low $|\vec{u}|$ indicates low hadronic activity $\rightarrow$ better precision
- Fits on signal regions
  - systematic uncertainties
  - results

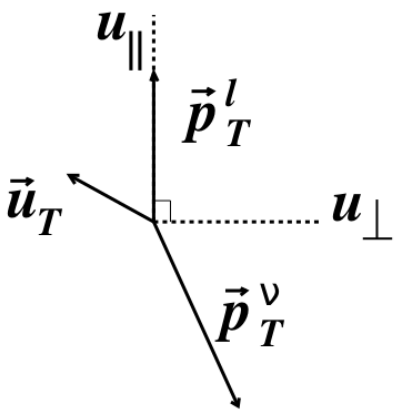

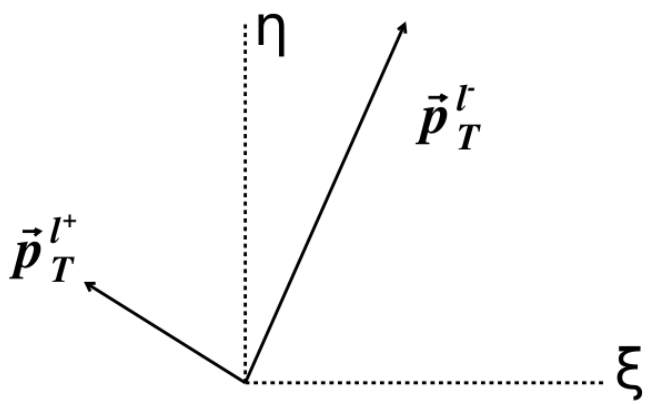

Selection, Signal, & Backgrounds

W Boson Event Selection & Background Estimation

- Single lepton triggers: loose lepton track and muon stub / calorimeter cluster requirements, with $p_{\mathrm{T}}^{\ell} > 18$ GeV
  - trigger efficiency ~100%
- Offline lepton selection:
  - Electron cluster $E_{\mathrm{T}} > 30$ GeV, track $p_{\mathrm{T}} > 18$ GeV
  - Muon track $p_{\mathrm{T}} > 30$ GeV
  - Loose identification requirements
- $30 < p_{\mathrm{T}}^{\ell} < 55$ GeV
- $30 < p_{\mathrm{T}}^{\mathrm{miss}} < 55$ GeV
- $60 < m_T < 100$ GeV
- $|\vec{u}| < 15$ GeV
- $N(\mathrm{W} \to \mu\nu/\mathrm{e}\nu) \sim 2.4/1.8$ M

$\mathrm{W} \to \mu\nu$ backgrounds

Source	Fraction (%)	δM_W (MeV) m_T fit	p_T^{μ} fit	p_T^{ν} fit
$Z/\gamma^* \to \mu\mu$	7.37 ± 0.10	1.6 (0.7)	3.6 (0.3)	0.1 (1.5)
$W \to \tau\nu$	0.880 ± 0.004	0.1 (0.0)	0.1 (0.0)	0.1 (0.0)
Hadronic jets	0.01 ± 0.04	0.1 (0.8)	-0.6 (0.8)	2.4 (0.5)
Decays in flight	0.20 ± 0.14	1.3 (3.1)	1.3 (5.0)	-5.2 (3.2)
Cosmic rays	0.01 ± 0.01	0.3 (0.0)	0.5 (0.0)	0.3 (0.3)
Total	8.47 ± 0.18	2.1 (3.3)	3.9 (5.1)	5.7 (3.6)

$\mathrm{W} \to \mathrm{e}\nu$ backgrounds

Source	Fraction (%)	δM_W (MeV) m_T fit	p_T^{e} fit	p_T^{ν} fit
$Z/\gamma^* \to ee$	0.134 ± 0.003	0.2 (0.3)	0.3 (0.0)	0.0 (0.6)
$W \to \tau\nu$	0.94 ± 0.01	0.6 (0.0)	0.6 (0.0)	0.6 (0.0)
Hadronic jets	0.34 ± 0.08	2.2 (1.2)	0.9 (6.5)	6.2 (−1.1)
Total	1.41 ± 0.08	2.3 (1.2)	1.1 (6.5)	6.2 (1.3)

Uncertainties due to background normalization and shape (in parentheses)

Simulation & Template Fitting

- Simulated events using a "Custom" Monte Carlo (MC)
  - aim to emulate particles through CDF detector in a quick, but accurate, manner
  - generate finely-spaced templates as a function of the fit variable
  - perform binned maximum-likelihood fits to the data
- Custom fast MC makes smooth templates
  - provides analysis control over key components of the simulation
- Extract W boson mass from 6 kinematic distributions:
  - e, μ & $m_T, p_T^{miss}, p_T^{\ell}$

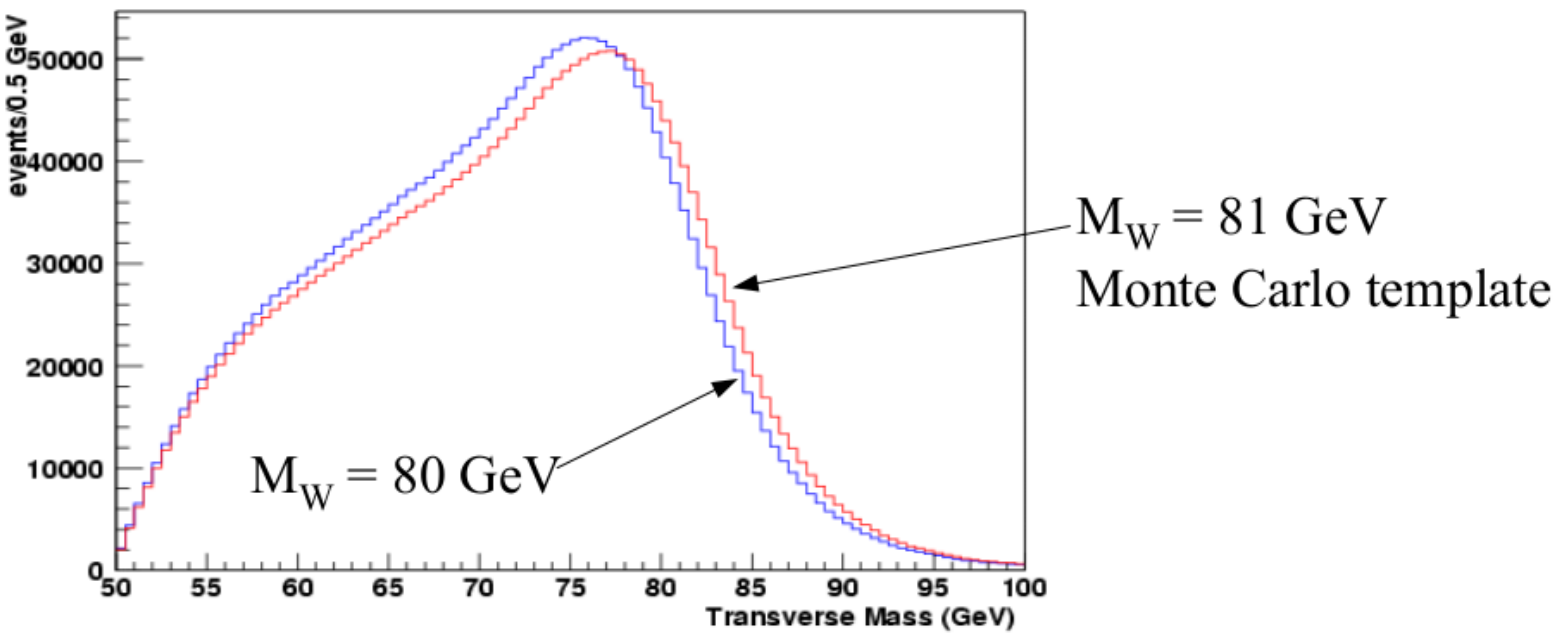

Theoretical Treatment

Generator-level Signal Simulation

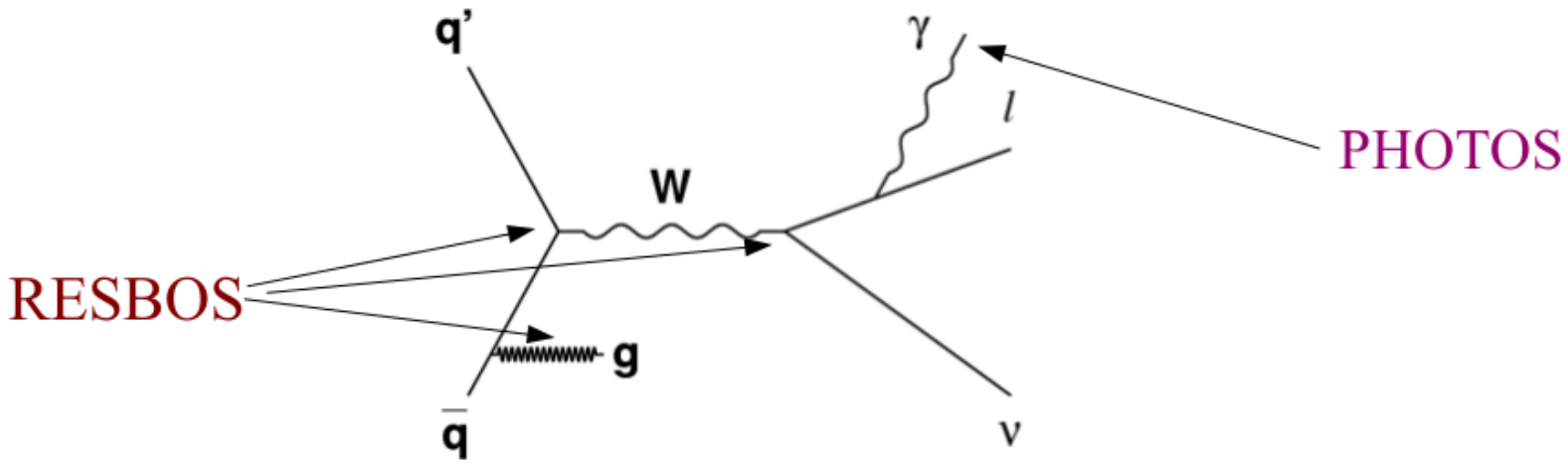

- Generator-level input for W & Z simulation provided by RESBOS
  - calculates differential production cross section, and p_{T}-dependent differential decay angular distribution
  - calculates boson p_{T} spectrum reliably over the relevant phase-space
- Custom fast Monte Carlo makes smooth templates
  - multiple radiative photons generated according to PHOTOS
- Very good agreement between data and RESBOS prediction
- Conscious decision to use RESBOS instead of newer MC generators

Constraining Boson p_{T} Spectrum (I)

- Fitting non-perturbative parameters in RESBOS using $p_{\mathrm{T}}^{\ell\ell}$ in Z boson events
  - uncertainties take into account both fit parameters and QCD coupling α_S
  - use azimuthal opening angle between leptons ($\phi^\star \sim p_{\mathrm{T}}^{\ell\ell}/m_{\ell\ell}$) as a check of the $p_{\mathrm{T}}^{\ell\ell}$ spectrum modeling
  - 1.8 MeV uncertainty from $p_{\mathrm{T}}^{\mathrm{Z}}$

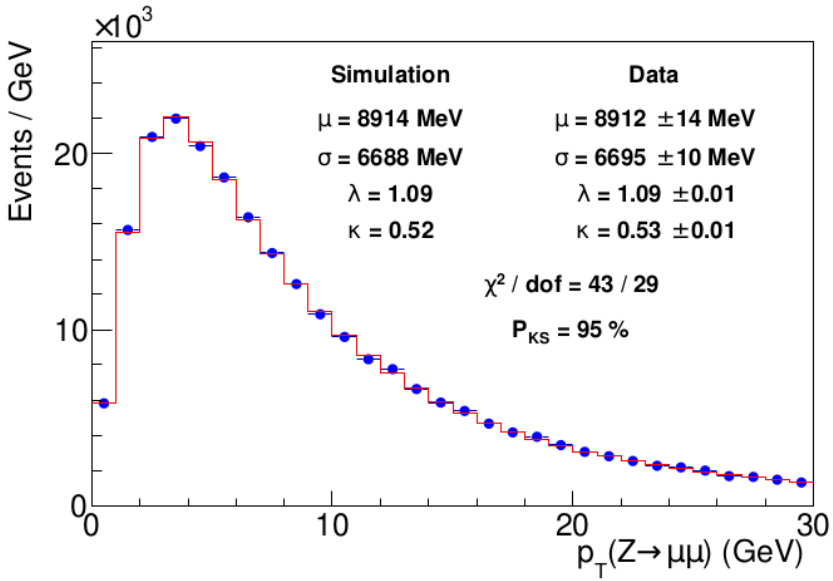

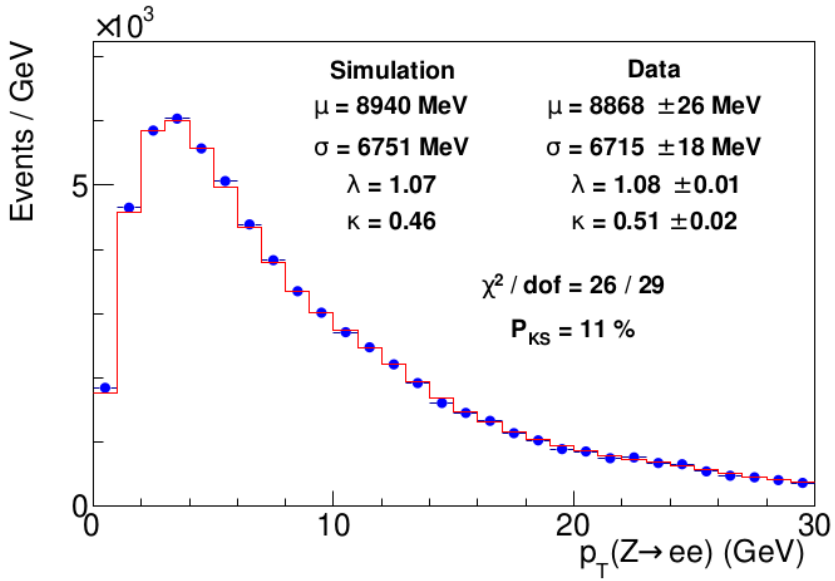

$$\phi^\star = \tan\left(\frac{\pi-\Delta\phi}{2}\right)\sin(\theta_\eta^*), \quad \cos(\theta_\eta^*) = \tanh\left(\frac{\Delta\eta}{2}\right)$$

Constraining Boson p_{T} Spectrum (II)

- Uncertainties in the $p_{\mathrm{T}}^{\mathrm{W}}/p_{\mathrm{T}}^{\mathrm{Z}}$ ratio estimated using DYQT program
  - triple-differential cross section calculation at NNLO in QCD
  - uncertainties computed as the envelope of the renormalization and factorization QCD scales
  - constraining the theoretical $p_{\mathrm{T}}^{\mathrm{W}}$ spectrum with CDF measured $p_{\mathrm{T}}^{\mathrm{W}}$ spectra, taking into account all the detector effects
  - 1.3 MeV uncertainty from $p_{\mathrm{T}}^{\mathrm{W}}/p_{\mathrm{T}}^{\mathrm{Z}}$

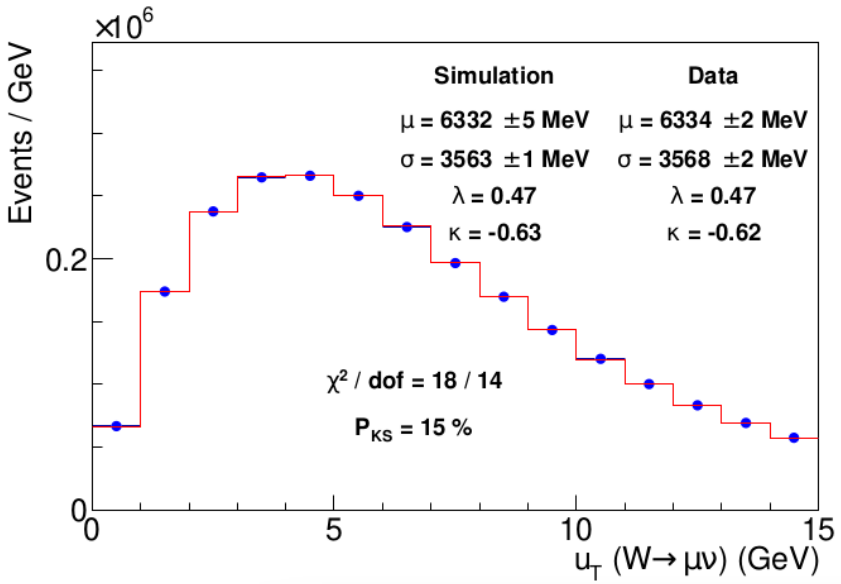

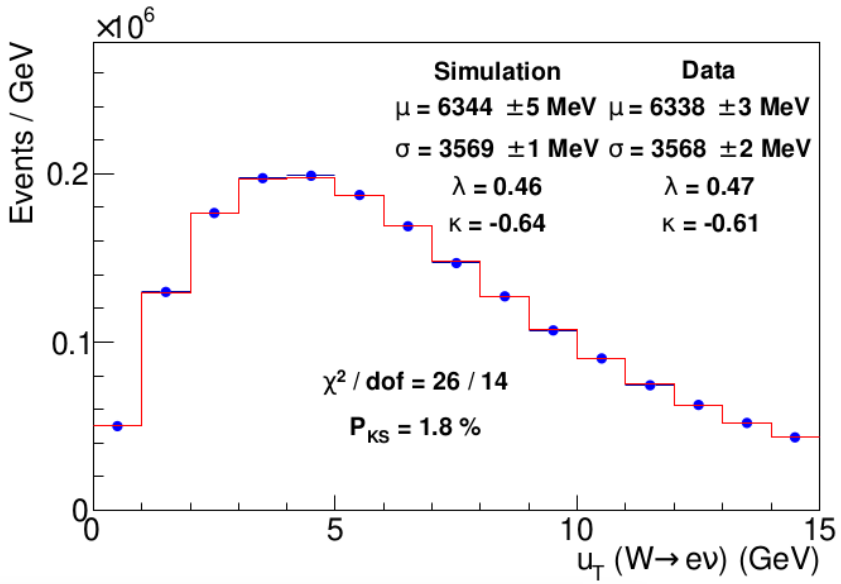

PDF Uncertainties

- At hadron colliders, distribution of longitudinal momentum of the interactions is determined by the PDFs describing the probability density of the fraction x of a hadron's momentum carried by an interacting parton
- Variations in the PDFs induce variations in the transverse kinematic distributions
- Used the NNPDF3.1 set at Next-Next-to-Leading order (NNLO) in QCD to quantify the PDF uncertainty from the global fit:
  - 3.9 MeV on the W boson mass
- For a consistency check, CT18, MMHT2014 AND NNPDF3.1 NNLO sets are compared
  - results agree with ± 2.1 MeV
- For a consistency check, ABMP16, CJ15, MMHT2014 AND NNPDF3.1 Next-to-Leading order sets are compared
  - results agree with ± 3.0 MeV

Calibration Measurements

Muon momentum calibration (I)

First step is the alignment of COT using cosmic muons

(AVK & CH, *NIM A* 762 (2014) pp 85-99)

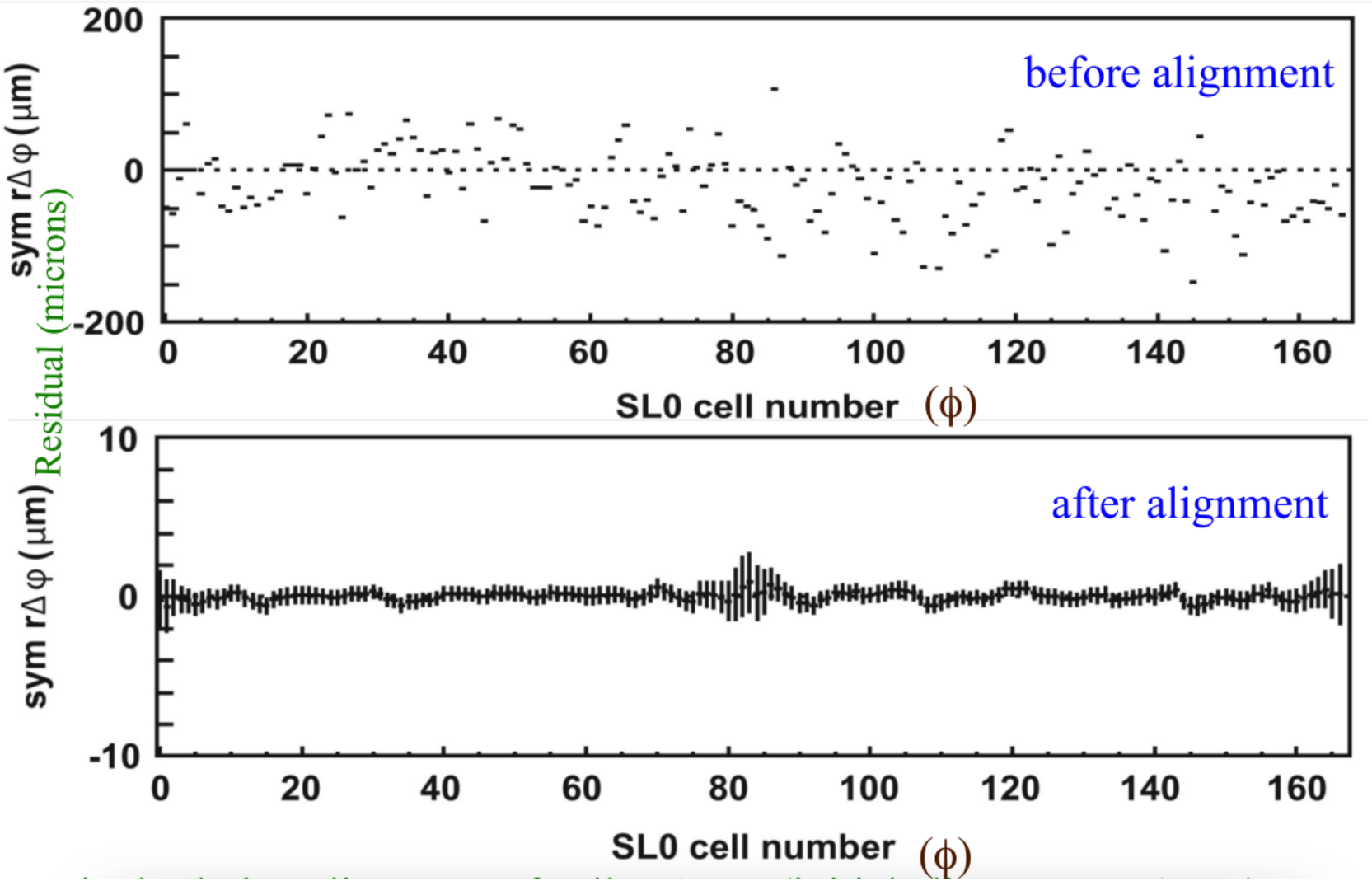

Rather flat distribution after this procedure

Muon momentum calibration (II)

- Second step is the calibration from $J/\psi \to \mu\mu$ decays
  - making use of PYTHIA simulation, together with a QED final-state radiation
- Third step is the calibration from $\Upsilon \to \mu\mu$ decays
  - beam constraint in the reconstruction of their decay products is added, reproducing the reconstruction procedure for tracks from W and Z bosons
- Results are combined to improve the precision

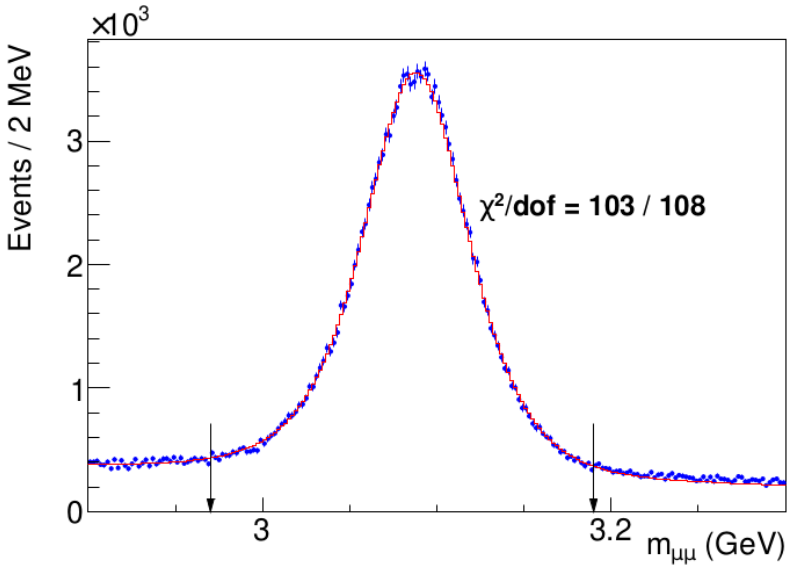

Source	J/ψ (ppm)	Υ (ppm)	Correlation (%)
QED	1	1	100
Magnetic field non-uniformity	13	13	100
Ionizing material correction	11	8	100
Resolution model	10	1	100
Background model	7	6	0
COT alignment correction	4	8	0
Trigger efficiency	18	9	100
Fit range	2	1	100
$\Delta p/p$ step size	2	2	0
World-average mass value	4	27	0
Total systematic	29	34	16 ppm
Statistical NBC (BC)	2	13(10)	0
Total	29	36	16 ppm

Muon momentum calibration (III)

Final step is the Z boson mass measurement

- $m_Z = 91192.2 \pm 6.4(\text{stat.}) \pm 4.0(\text{syst.})$ MeV
  - consistent with PDG value $m_Z = 91187.6 \pm 2.1(\text{syst.})$ MeV
- Combine all measurements into a final charged-track momentum scale
- $|\Delta p/p| = -1389 \pm 25$ ppm, $\Delta(m_W) \sim 2$ MeV

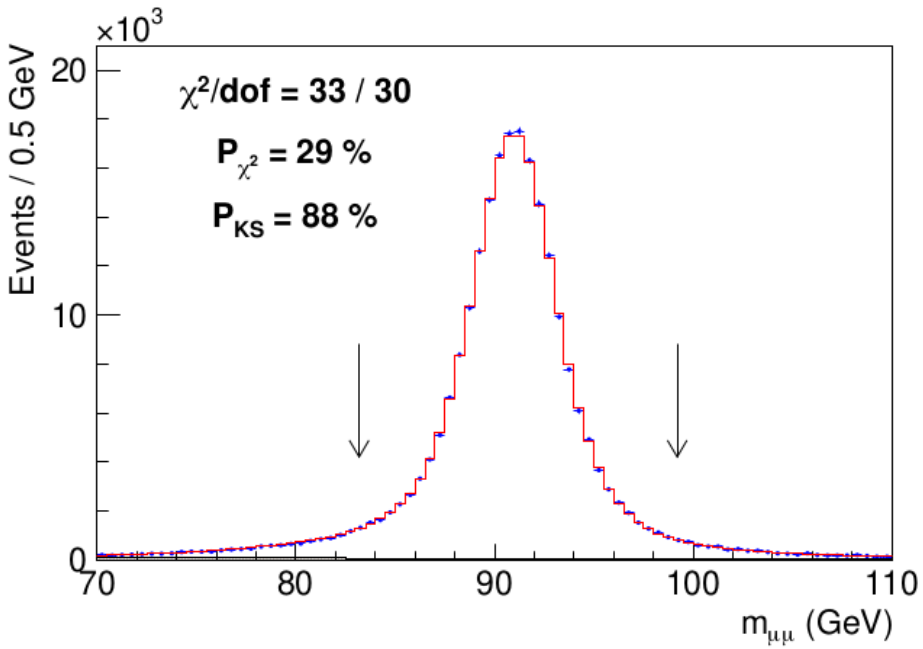

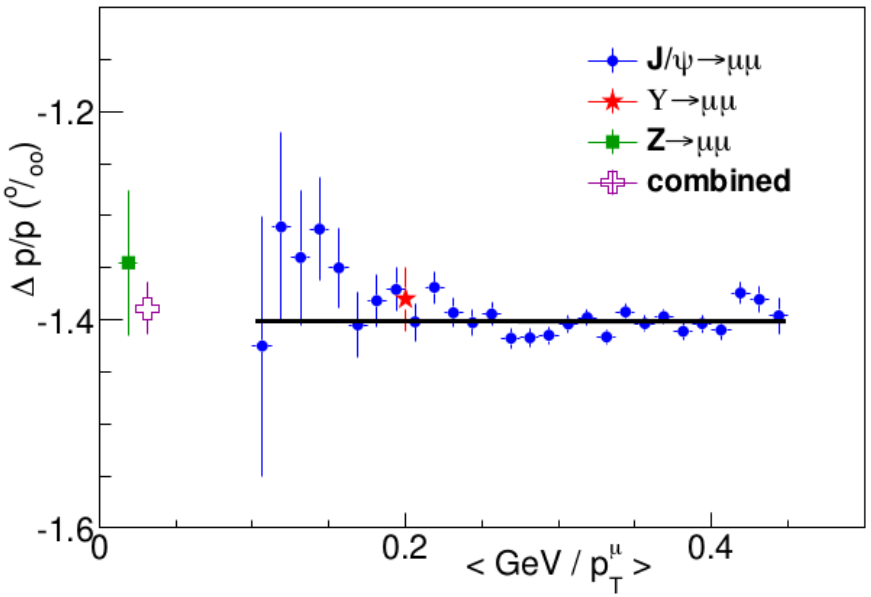

Electron momentum calibration (I)

- Electron radiates bremsstrahlung photons as it traverses the tracking volume, degrading its track momentum resolution
- Therefore, the higher-resolution calorimeter energy measurement is used
- Calibration of p is transferred to the calorimeter energy E by fitting E/p

First step is the correction for response variations in space and time

Fit ratio of calorimeter energy to track momentum to correct each tower in η
Use mean E/p to remove time dependence & response variations in tower

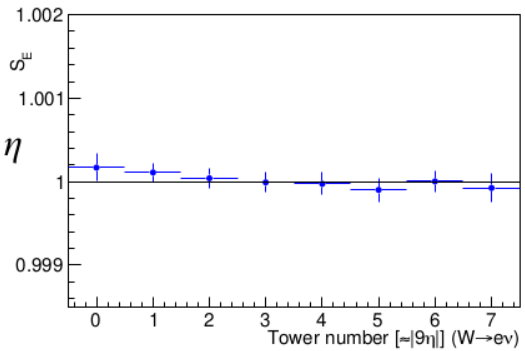

Second step is the calibration of the energy scale using E/p

Custom parameterized GEANT simulation of calorimeter

AVK & CH, 1308.2025 & NIM A 729, 25 (2013)

Use E/p and tail fits to simulate osmall non-linear energy response and variations in calorimeter thickness

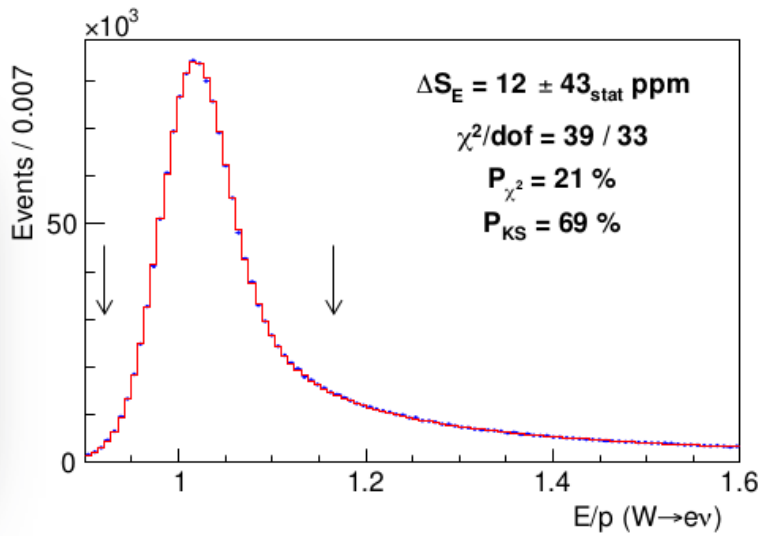

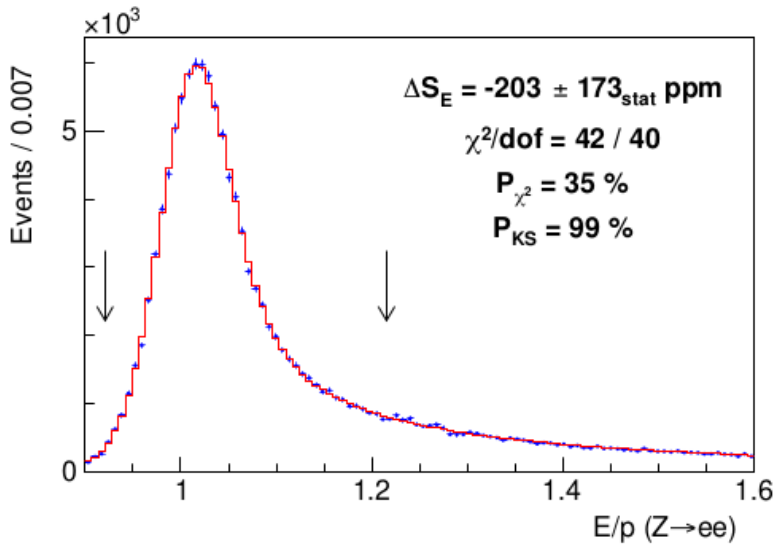

Electron momentum calibration (II)

Final step is the Z boson mass measurement

- $m_{\mathrm{Z}}(\text{full}) = 91194.3 \pm 13.8(\text{stat.}) \pm 7.6(\text{syst.})\ \mathrm{MeV}$
- $m_{\mathrm{Z}}(\text{track only}) = 91215.2 \pm 22.4(\text{total})\ \mathrm{MeV}$
- Total calibration factor: -14 ± 72 ppm, $\Delta(m_{\mathrm{W}}) \sim 6\ \mathrm{MeV}$

Full

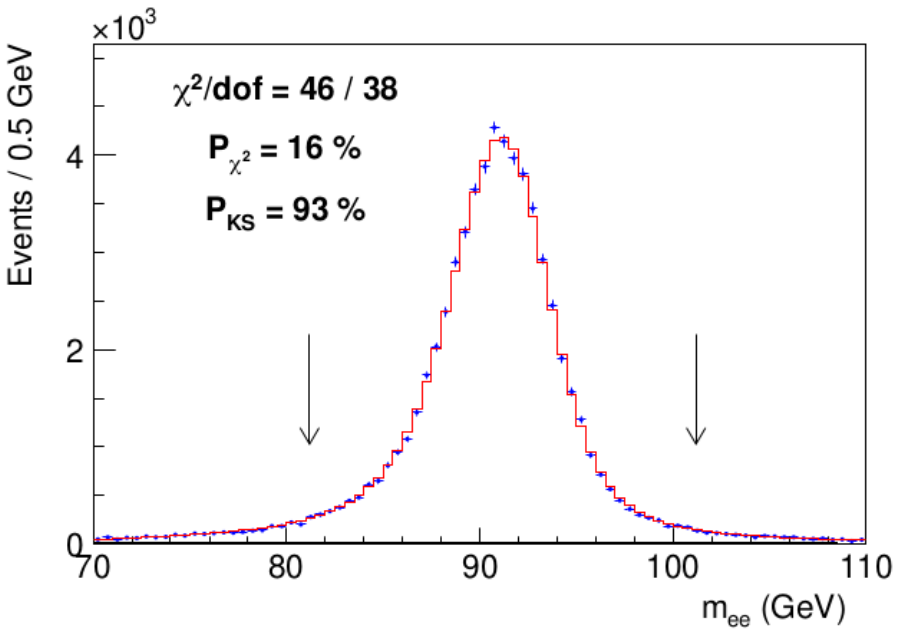

Track only

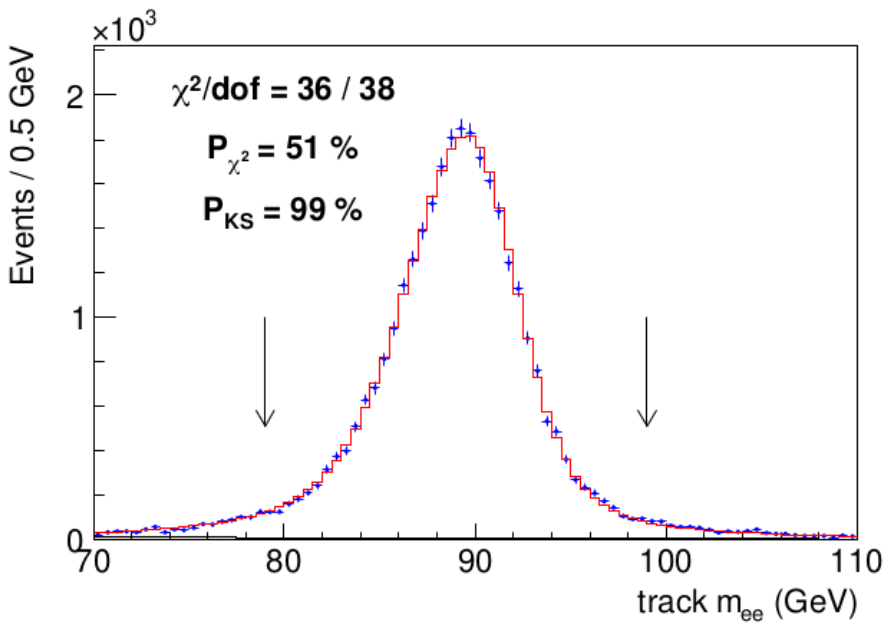

Constraining Hadronic Recoil Model

- Exploit similarity in production and decay of W and Z bosons
- Detector response model for hadronic recoil tuned using p_{T}-balance in $\mathrm{Z} \to \ell\ell$ events
- Transverse momentum of Hadronic recoil (u) calculated as 2-vector sum over calorimeter towers

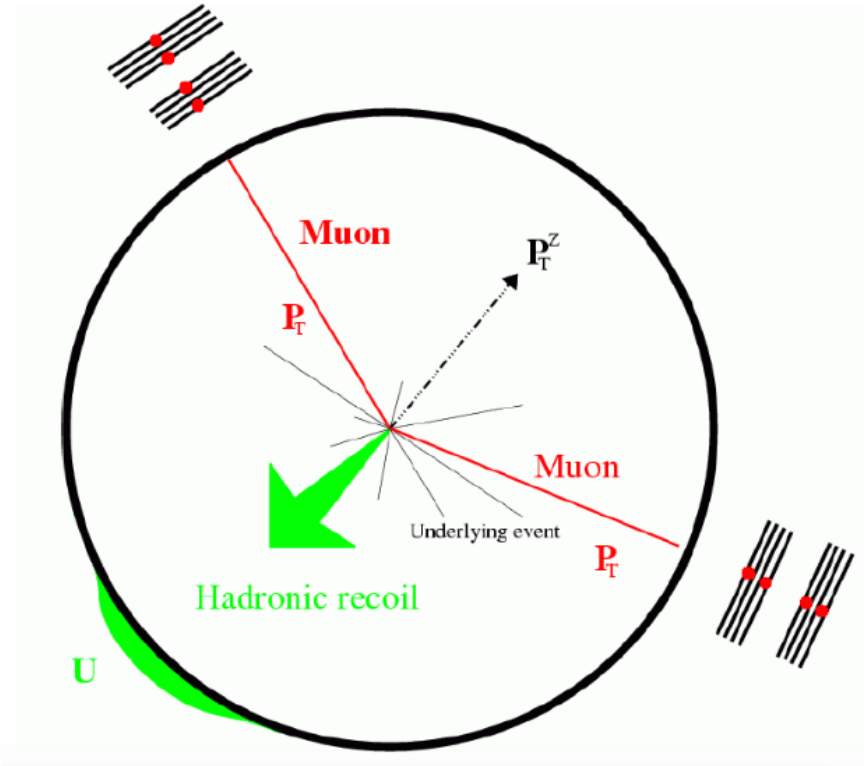

Graph courtesy T. Dorigo

Recoil Calibration

- First step is the alignment of the calorimeters
  - flat response as a function of $\phi_{\vec{p}_{\mathrm{T}}^{\mathrm{miss}}}$
  - modeled using minimum-bias data
- Second step is the reconstruction of the recoil
  - remove calorimeter towers traversed by identified leptons
- Third step is the calibration of the recoil response
  - Recoil scale $R = u_{meas}/u_{true}$
  - use ratio of recoil magnitude to $p_{\mathrm{T}}^{\mathrm{Z}}$ along direction of $p_{\mathrm{T}}^{\mathrm{Z}}$

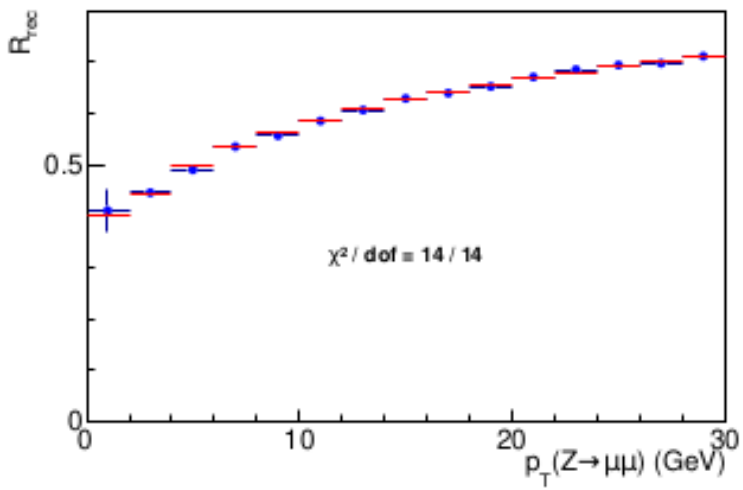

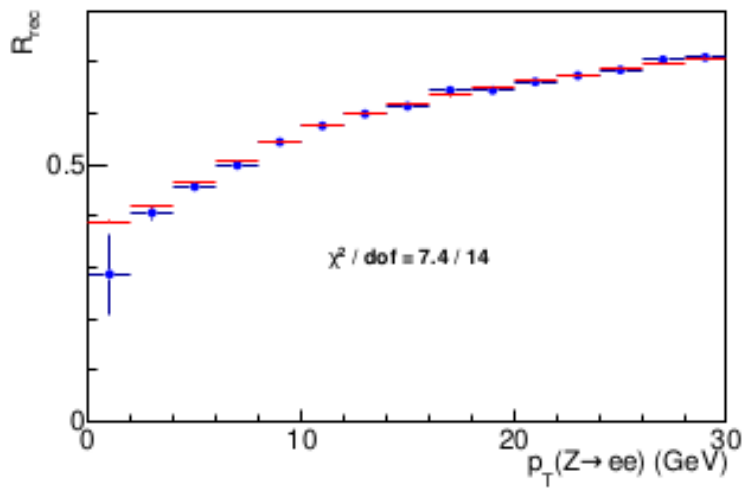

- Fourth step is the calibration of the recoil resolution
  - takes into account additional soft-jet production

Recoil Validation

W boson recoil distributions validate the model

Most important is the recoil projected along the charged-lepton's momentum ($u_{||}$)

$$m_T \approx 2p_T\sqrt{1+u_{||}/p_T} \approx 2p_T + u_{||}.$$

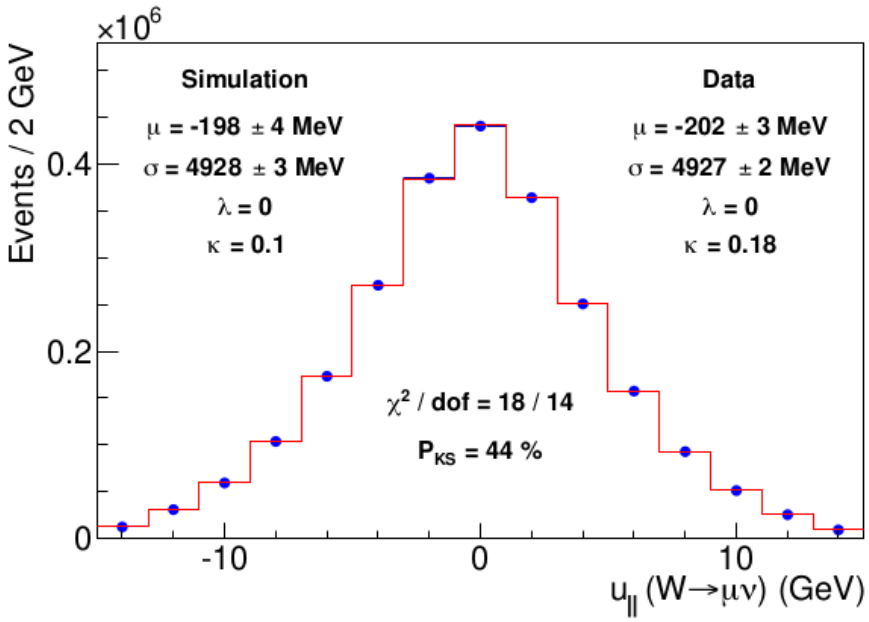

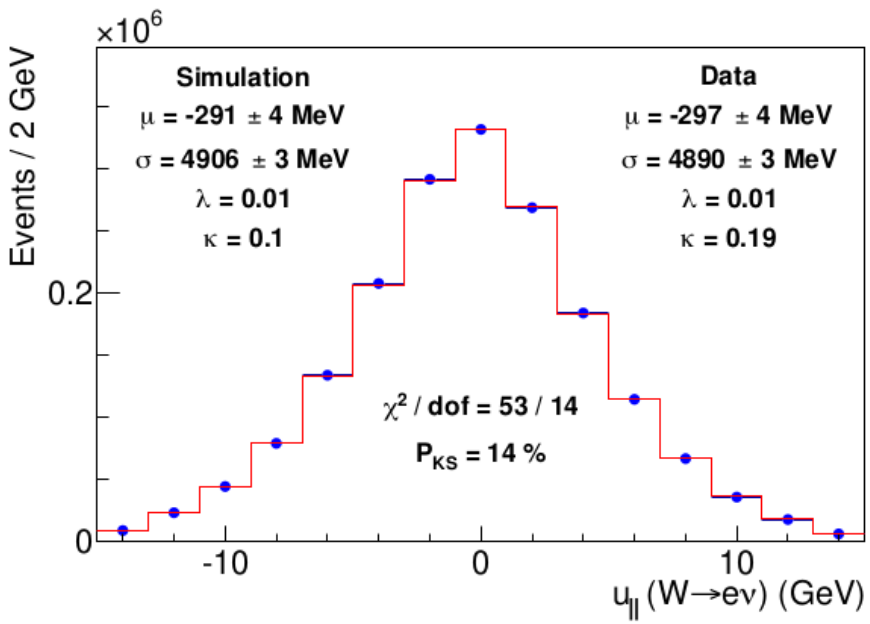

Uncertainties & Fits on Signal Regions

Systematic Uncertainties: the Name of the Game

Method or technique	impact	section of paper
Detailed treatment of parton distribution functions	+3.5 MeV	IV A
Resolved beam-constraining bias in CDF reconstruction	+10 MeV	VI C
Improved COT alignment and drift model [65]	uniformity	VI
Improved modeling of calorimeter tower resolution	uniformity	III
Temporal uniformity calibration of CEM towers	uniformity	VII A
Lepton removal procedure corrected for luminosity	uniformity	VIII A
Higher-order calculation of QED radiation in J/ψ and Υ decays	accuracy	VI A & B
Modeling kurtosis of hadronic recoil energy resolution	accuracy	VIII B 2
Improved modeling of hadronic recoil angular resolution	accuracy	VIII B 3
Modeling dijet contribution to recoil resolution	accuracy	VIII B 4
Explicit luminosity matching of pileup	accuracy	VIII B 5
Modeling kurtosis of pileup resolution	accuracy	VIII B 5
Theory model of p_T^W/p_T^Z spectrum ratio	accuracy	IV B
Constraint from p_T^W data spectrum	robustness	VIII B 6
Cross-check of p_T^Z tuning	robustness	IV B

- Large number of improvements w.r.t. previous analysis iteration

All Fit Uncertainties (MeV)

Source of systematic uncertainty	m_T fit			p_T^ℓ fit			p_T^ν fit		
	Electrons	Muons	Common	Electrons	Muons	Common	Electrons	Muons	Common
Lepton energy scale	5.8	2.1	1.8	5.8	2.1	1.8	5.8	2.1	1.8
Lepton energy resolution	0.9	0.3	-0.3	0.9	0.3	-0.3	0.9	0.3	-0.3
Recoil energy scale	1.8	1.8	1.8	3.5	3.5	3.5	0.7	0.7	0.7
Recoil energy resolution	1.8	1.8	1.8	3.6	3.6	3.6	5.2	5.2	5.2
Lepton $u_{\|\|}$ efficiency	0.5	0.5	0	1.3	1.0	0	2.6	2.1	0
Lepton removal	1.0	1.7	0	0	0	0	2.0	3.4	0
Backgrounds	2.6	3.9	0	6.6	6.4	0	6.4	6.8	0
p_T^Z model	0.7	0.7	0.7	2.3	2.3	2.3	0.9	0.9	0.9
p_T^W/p_T^Z model	0.8	0.8	0.8	2.3	2.3	2.3	0.9	0.9	0.9
Parton distributions	3.9	3.9	3.9	3.9	3.9	3.9	3.9	3.9	3.9
QED radiation	2.7	2.7	2.7	2.7	2.7	2.7	2.7	2.7	2.7
Statistical	10.3	9.2	0	10.7	9.6	0	14.5	13.1	0
Total	13.5	11.8	5.8	16.0	14.1	7.9	18.8	17.1	7.4

- m_T variable more relevant than at LHC
  - superior recoil performance, in spite of better LHC detectors
  - higher $\sqrt{s}$ at the LHC implies larger hadronic activity
- Combined fits by means of the best linear unbiased estimator (BLUE)

Systematic Uncertainties: Old vs. New Result

Source	Final CDF Run 2 (MeV)	First CDF Run 2 (MeV)
Lepton energy scale & resolution	3.2	7
Recoil energy scale & resolution	2.2	6
Lepton efficiency & removal	1.3	2
Backgrounds	3.3	3
$p_{\mathrm{T}}^{\mathrm{Z}}$ & $p_{\mathrm{T}}^{\mathrm{W}}$ models	2.2	5
PDFs	3.9	10
QED radiation	2.7	4
Statistical	6.4	12
Total	9.4	19

- Statistical precision of the measurement from the four times larger sample is improved by almost a factor of two
- Analysis improvements have also been incorporated:
  - COT alignment and drift model and the uniformity of the calorimeter response
  - accuracy and robustness of the detector response and resolution model in the simulation
  - theoretical inputs to the analysis have been updated
- Notice previous measurement should change by $+13.5$ MeV

Systematic Uncertainties: Comparison with ATLAS Result

Source	Final CDF Run 2 (MeV)	ATLAS (MeV)
Lepton uncertainties	3.5	9.2
Recoil energy scale & resolution	2.2	2.9
Backgrounds	3.3	4.5
Model theoretical uncertainties	3.5	9.9
PDFs	3.9	9.2
Statistical	6.4	6.8
Total	9.4	18.5

- Similar data sample, i.e., similar statistical precision
- Larger experimental and theoretical uncertainties in ATLAS result
- Larger dataset and/or additional fitting variables at LHC to reach CDF uncertainties

Final Fit Distributions

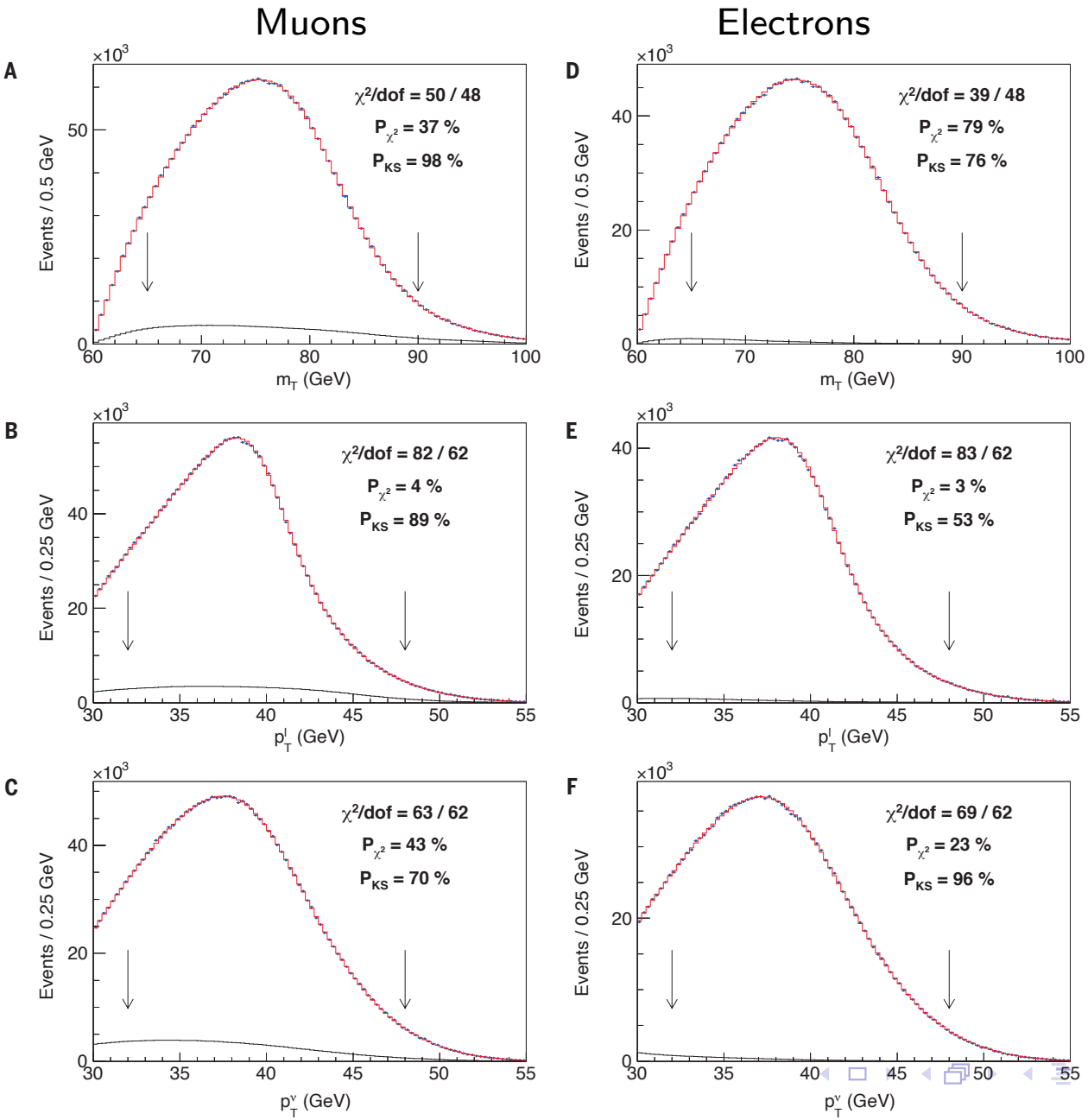

Results & Discussion

Fit Results

Distribution	W-boson mass (MeV)	χ^2/dof
$m_T(e,\nu)$	$80\,429.1 \pm 10.3_{\text{stat}} \pm 8.5_{\text{syst}}$	39/48
$p_T^{\ell}(e)$	$80\,411.4 \pm 10.7_{\text{stat}} \pm 11.8_{\text{syst}}$	83/62
$p_T^{\nu}(e)$	$80\,426.3 \pm 14.5_{\text{stat}} \pm 11.7_{\text{syst}}$	69/62
$m_T(\mu,\nu)$	$80\,446.1 \pm 9.2_{\text{stat}} \pm 7.3_{\text{syst}}$	50/48
$p_T^{\ell}(\mu)$	$80\,428.2 \pm 9.6_{\text{stat}} \pm 10.3_{\text{syst}}$	82/62
$p_T^{\nu}(\mu)$	$80\,428.9 \pm 13.1_{\text{stat}} \pm 10.9_{\text{syst}}$	63/62
combination	$80\,433.5 \pm 6.4_{\text{stat}} \pm 6.9_{\text{syst}}$	7.4/5

- Consistency between two channels and three kinematic fits
- Great robutness from the experimental point of view, since several categories are largely independent to each other

Consistency Checks

Combination	m_T fit		p_T^ℓ fit		p_T^ν fit		Value (MeV)	χ^2/dof	Probability (%)
	Electrons	Muons	Electrons	Muons	Electrons	Muons			
m_T	✓	✓					$80\,439.0 \pm 9.8$	1.2 / 1	28
p_T^ℓ			✓	✓			$80\,421.2 \pm 11.9$	0.9 / 1	36
p_T^ν					✓	✓	$80\,427.7 \pm 13.8$	0.0 / 1	91
m_T & p_T^ℓ	✓	✓	✓	✓			$80\,435.4 \pm 9.5$	4.8 / 3	19
m_T & p_T^ν	✓	✓			✓	✓	$80\,437.9 \pm 9.7$	2.2 / 3	53
p_T^ℓ & p_T^ν			✓	✓	✓	✓	$80\,424.1 \pm 10.1$	1.1 / 3	78
Electrons	✓		✓		✓		$80\,424.6 \pm 13.2$	3.3 / 2	19
Muons		✓		✓		✓	$80\,437.9 \pm 11.0$	3.6 / 2	17
All	✓	✓	✓	✓	✓	✓	$80\,433.5 \pm 9.4$	7.4 / 5	20

Fit difference	Muon channel	Electron channel
$M_W(\ell^+) - M_W(\ell^-)$	$-7.8 \pm 18.5_{\text{stat}} \pm 12.7_{\text{COT}}$	$14.7 \pm 21.3_{\text{stat}} \pm 7.7^{\text{E/p}}_{\text{stat}}$ $(0.4 \pm 21.3_{\text{stat}})$
$M_W(\phi_\ell > 0) - M_W(\phi_\ell < 0)$	$24.4 \pm 18.5_{\text{stat}}$	$9.9 \pm 21.3_{\text{stat}} \pm 7.5^{\text{E/p}}_{\text{stat}}$ $(-0.8 \pm 21.3_{\text{stat}})$
$M_Z(\text{run} > 271100) - M_Z(\text{run} < 271100)$	$5.2 \pm 12.2_{\text{stat}}$	$63.2 \pm 29.9_{\text{stat}} \pm 8.2^{\text{E/p}}_{\text{stat}}$ $(-16.0 \pm 29.9_{\text{stat}})$

- Consistent results using independent samples
- For the spatial and time dependence of the electron channel fit result, we show the dependence with (without) the corresponding cluster energy calibration using the subsample E/p fit

Summary

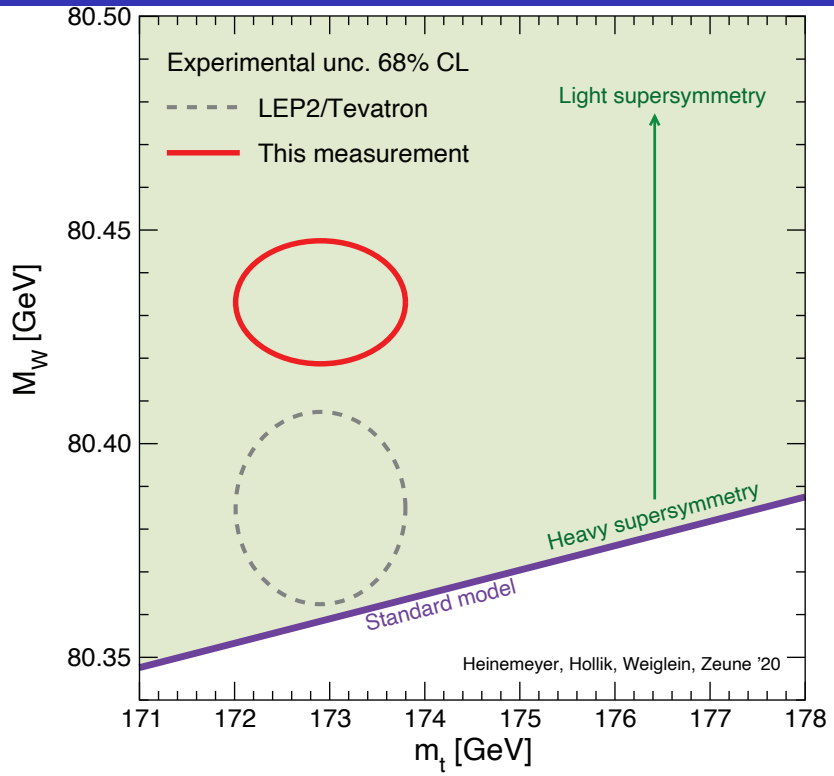

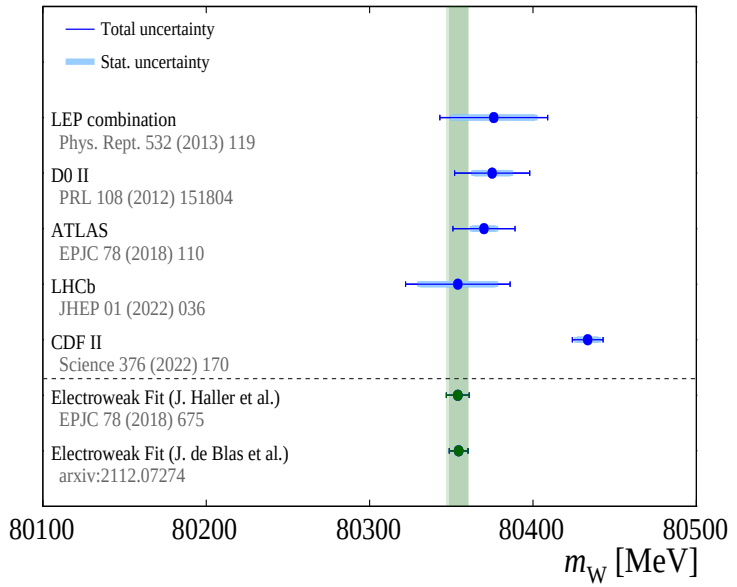

- Impressive precision by CDF on the W boson mass measurement, still with a large statistical component!
- Result of >20 years of experience with the CDF II detector
- 6 independent, partially correlated, measurements agree (electrons/muons - $p_{\mathrm{T}}^{\ell}/p_{\mathrm{T}}^{\mathrm{miss}}/m_T$)
- Sizable tension with the SM EW fit predictions ($> 5\sigma$?) and with other experiments ($\sim 3\sigma$?)

Usual Q&A

- Do old and new CDF results agree?
  - after taking into account the $+13.5\ \mathrm{MeV}$ shift, results agree within $\sim 1.5\ \sigma$
- Why using RESBOS?
  - was extensively used and studied by more than 15 years
  - both generators and PDF sets will be further studied for the Tevatron+LHC combination
- Why PDF uncertainties got reduced?
  - because a new NNLO PDF set (NNPDF3.1) following the most up to date prescription was used
- Was the result modified after unblinding the data?
  - no, the analysis was reviewed by a large number of people blinded, and results were not modified after looking at the data
- Do you think LHC measurement could reach an uncertainty below $10\ \mathrm{MeV}$?
  - possibly so, but it will require patience

Implications for LHC

- First of all, a grand combination is on-going
  - central values may change if different theoretical treatments are followed, stay tuned
- New LHC W boson mass measurements are more welcome than ever
  - hope this is a very high priority for experiments, but also for individuals
- Recently released new precise top quark mass measurement from CMS, $m_{\text{top}} = 171.77 \pm 0.38\ \mathrm{GeV}$, unfortunately (or fortunately) goes in the "wrong" way for the SM
  - A larger W boson mass and a smaller top quark mass increases the tension with the SM
- Plenty of new physics explanations appearing in the market
  - non-zero anomalous couplings is the first way to see it
  - should study if other anomalies are consistent with these results
- Finding rare fully hadronic W boson decays in Run 3 would give an option to measure the W boson mass using the HL-LHC data set
  - $\mathrm{W} \to \pi\gamma,\ \pi\pi\pi$ decays have been searched for in Run 2

Back-Up Slides

Documentation

- First Run 2 CDF paper: Phys. Rev. Lett. 108 (2012) 151803, arXiv:1203.0275
- Full Run 2 CDF paper: Science 376, 170 (2022), DOI: 10.1126/science.abk1781
- Identification of cosmic rays using drift chamber hit timing: A. Kotwal, H. Gerberich, C. Hays, NIM A 506, 110 (2003)
- Drift Chamber Alignment using Cosmic Rays: A. Kotwal, C. Hays, NIM A 762 (2014)
- RESBOS: C. Balazs, C.-P. Yuan, PRD56, 5558 (1997)
- PHOTOS: P. Golonka, Z. Was, Eur. J. Phys. C 45, 97 (2006)
- RESBOS2 and the CDF W Mass Measurement: arXiv:2205.02788
- ATLAS W boson mass measurement: Eur. Phys. J. C 78 (2018) 110
- LHCb W boson mass measurement: JHEP 01 (2022) 036

Basic Analysis Principles

Measurement performed by a small dedicated team for over 10 years, with a good number of reviewers following them

- Robustness:
  - constrain the same parameters in as many different ways as possible
  - take as much time as it takes
- Precision:
  - combine independent measurements after showing consistency
  - push analyses as hard as reasonable, but using well-known procedures
- Minimize bias:
  - blinded Z and W boson mass measurements

Little Disclaimer

- While not a main author in the CDF analysis, have been involved in electroweak measurements for a long time
- Worked on W boson physics at the DELPHI experiment
  - σ_{WW} and W boson branching ratio measurements
- CDF member since 2001, main involvement in B physics
  - $B_{s/d}$ mixing and $sin(2\beta_s)$ measurements
  - participated in the review of the W boson mass measurement
- CMS member since 1999, although actively since 2006
  - worked on Higgs, exotica, and electroweak physics
  - performed several multiboson and vector boson scattering measurements
  - performed detailed Z boson differential measurements, which are used to tune the CMS simulation towards the first W boson mass measurement
  - currently, co-coordinator of the standard model physics group

Is it 7 σ Away from SM? (Personal View)

- It is "several" standard deviation w.r.t. SM fit
- Systematic uncertainties evaluation is an art, the finest art for a high precision measurement
  - result with muons is higher than the result with electrons, still consistent to each other
  - custom simulation instead of full GEANT4 simulation?
  - modifying fit ranges show some trends within ± 10 MeV
  - momentum scale determination driven by studies of low-mass resonances
  - making use of the most up to date RESBOS version may give a variation of 10 MeV at most
- The items listed above may give additional uncertainties, going 9.4 MeV to $\sim$ 12.6 MeV would not change my view
  - Δ(PDF) : 3.9 $\rightarrow$ 5.3 MeV (from the envelop of all PDF sets)
  - $\Delta(p_{\mathrm{T}}^{\mu})$: 2.1 $\rightarrow$ 5.2 MeV (from m_{Z} measurement)
  - $\Delta(p_{\mathrm{T}}^{\mathrm{V}})$: 3.5 $\rightarrow$ 7.0 MeV (from RESBOS2 studies)

Most Recent Measurements: ATLAS /LHCb / CDF

	ATLAS	LHCb	CDF
Collider	pp	pp	$\mathrm{p\bar{p}}$
$\sqrt{s}$	7	13	1.96
$\mathcal{L}$	4.1–4.6	1.7	8.8
$N_{pileup} \sim$	9	2	3
Final states	e/μ	μ	e/μ
Fit variables	m_T, p_{T}^{ℓ}	q/p_{T}^{ℓ}, $p_{\mathrm{T}}^{\mathrm{miss}}$	m_T, p_{T}^{ℓ}, $p_{\mathrm{T}}^{\mathrm{miss}}$
$p_{\mathrm{T}}^{\ell} > (\mathrm{GeV})$	30	28	30
$p_{\mathrm{T}}^{\ell} < (\mathrm{GeV})$	50	52	55
$\eta^{\ell} >$	-2.5	2.2	-1.0
$\eta^{\ell} <$	2.5	4.4	1.0
$p_{\mathrm{T}}^{\mathrm{miss}} > (\mathrm{GeV})$	30	N/A	30
$m_T > (\mathrm{GeV})$	60	N/A	60
$m_T < (\mathrm{GeV})$	100	N/A	100
$u_T < (\mathrm{GeV})$	15	N/A	15
Selected events $\sim$	13.7M	2.4M	4.2M
MC generator	POWHEG-PYTHIA 8	POWHEG-PYTHIA 8	RESBOS
PDF set	NNPDF3.0	NNPDF3.1	NNPDF3.1

Custom Monte Carlo Detector Simulation

- A complete detector simulation of all quantities measured in the data
- First-principles simulation of tracking
  - tracks and photons propagated through a high-resolution 3-D lookup table of material properties for silicon detector and COT
  - at each material interaction, calculate
    - ionization energy loss according to detailed formulae and Landau distribution
    - generate bremsstrahlung photons down to 0.4 MeV, using detailed cross section and spectrum calculations
    - simulate photon conversion and Compton scattering
    - propagate bremsstrahlung photons and conversion electrons
    - simulate multiple Coulomb scattering
  - deposit and smear hits on COT wires, perform full helix fit including optional beam-constraint
- 3-D Material Map in Simulation
  - tuned based on studies of inclusive photon conversions
  - radiation lengths vs (ϕ, z) at different radii shows localized nature of material distribution
  - include dependence on type of material via soft bremsstrahlung

Calorimeter Simulation for Electrons and Photons

- Distributions of lost energy calculated using detailed GEANT4 simulation of calorimeter, tuned on data
  - leakage into hadronic calorimeter
  - absorption in the coil
  - dependence on incident angle and E_T
- Energy-dependent gain (non-linearity) parameterized and fit from data
- Energy resolution: fixed sampling term and tunable constant term
  - constant terms are fit from the width of E/p peak and $\mathrm{Z} \rightarrow \mathrm{ee}$ mass peak
- Studied consistency of radiative material model
  - excellent description of E/p spectrum tail
- Measurement of EM calorimeter non-linearity
  - perform E/p fit-based calibration in bins of electron E_T
- EM Calorimeter Uniformity
  - check uniformity of energy scale in bins of electron pseudo-rapidity

Lepton Resolutions in the Custom Simulation

- Tracking resolution parameterized by
  - radius-dependent drift chamber hit resolution, $\sigma_h \sim 150\mu m$
  - beamspot size, $\sigma_b \sim 36\mu m$
  - tuned on the widths of the $\mathrm{Z} \to \mu\mu$ (beam-constrained) and $\Upsilon \to \mu\mu$ (constrained and non-beam constrained) mass peaks
    - $\Delta m_{\mathrm{W}} = 0.3\ \mathrm{MeV}$ (muons)
- Electron cluster resolution parameterized by
  - sampling term $\sim 12.6\%/\sqrt{E_T}$
  - constant term $\sim 0.76\%$
  - tuned on the width of E/p peak and $\mathrm{Z} \to \mathrm{ee}$ mass peak
    - $\Delta m_{\mathrm{W}} = 0.9\ \mathrm{MeV}$ (electrons)

Production & Decay Models

- W and Z bosons generated using the CTEQ6M PDFs extracted at NLO in QCD, and the RESBOS generator, which uses perturbative QCD and a parametrization of nonperturbative QCD effects to calculate boson production and decay kinematics
  - PHOTOS is used to simulate internal bremsstrahlung
  - future improvements or corrections in any relevant theoretical modeling may alter the result
- Simulation is reweighted to use NNPDF3.1 at NNLO in QCD as default PDF
- NNPDF3.1 set also used to quantify the PDF uncertainty from the global fit
  - used a set of 25 symmetric eigenvectors
- Missing higher-order QCD effects
  - varying factorization and renormalization scales in RESBOS
  - comparing two event generators
  - estimated uncertainty $\sim 0.4\ \mathrm{MeV}$ (neglected)

Uncertainties in QED Calculations

- Extensive comparisons between PHOTOS and HORACE
  - Comparing multi-photon final state radiation algorithms
  - Including multi-photon radiation from all charged lines (HORACE), and consistency with exact one-photon calculation
- Extensive studies performed on uncertainties arising from
  - leading logarithm approximation
  - multi-photon calculation
  - higher order soft and virtual corrections
  - electron-positron pair creation
  - QED/QCD interference
  - dependence on electroweak parameters/scheme
- Total systematic uncertainty due to QED radiation on W mass measurement: $\underline{2.7\ \mathrm{MeV}}$
  - tripling the energy cutoff E_{T} threshold: $1\ \mathrm{MeV}$
  - comparison of FSR from the PHOTOS and HORACE: $0.7\ \mathrm{MeV}$
  - NLO QED calculation from HORACE: $+4 \pm 2\ \mathrm{MeV}$
  - HORACE simulation uncertainty: $1\ \mathrm{MeV}$
  - internal photon conversion uncertainty: $1\ \mathrm{MeV}$

W & Z Boson p_{T} Spectrum (I)

- Fitting non-perturbative parameters in RESBOS using $p_{\mathrm{T}}^{\ell\ell}$ in Z boson events
  - uncertainties take into account both fit parameters and QCD coupling α_S
  - $(0.7, 2.3, 0.9)$ MeV for (m_T, p_{T}^{ℓ}, $p_{\mathrm{T}}^{\mathrm{miss}}$) fits

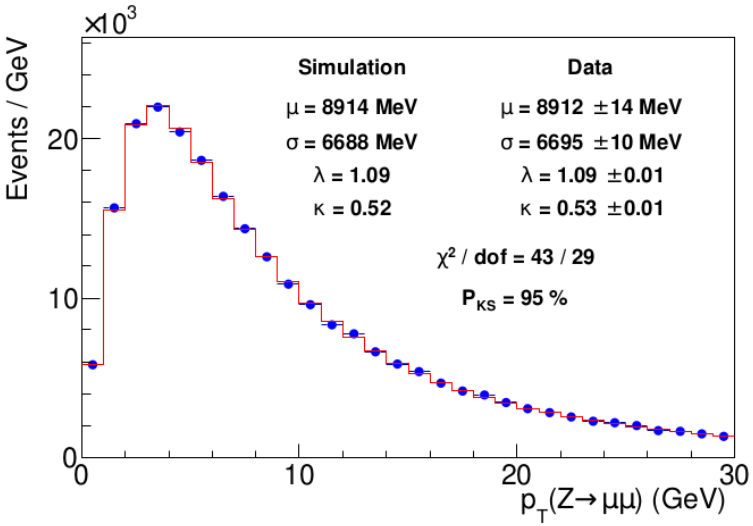

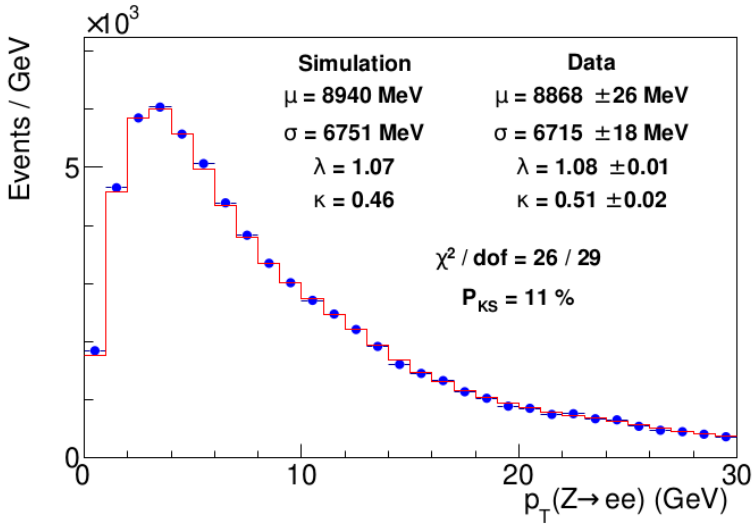

- Use azimuthal opening angle between leptons ($\phi^{\star}$) as a check of the $p_{\mathrm{T}}^{\ell\ell}$ spectrum modeling

W & Z Boson p_{T} Spectrum (II)

- Uncertainties in the $p_{\mathrm{T}}^{\mathrm{W}}/p_{\mathrm{T}}^{\mathrm{Z}}$ ratio estimated using DYQT program
  - triple-differential cross section calculation at NNLO in QCD
  - uncertainties computed as the envelope of the renormalization and factorization QCD scales
  - $(3.5, 10.1, 3.9)$ MeV for $(m_T,\ p_{\mathrm{T}}^{\ell},\ p_{\mathrm{T}}^{\mathrm{miss}})$ fits
- These uncertainties reduced a factor of 4.4 by constraining the theoretical $p_{\mathrm{T}}^{\mathrm{W}}$ spectrum with CDF measured $p_{\mathrm{T}}^{\mathrm{W}}$ spectra, taking into account all the detector effects
  - $(0.8, 2.3, 0.9)$ MeV for $(m_T,\ p_{\mathrm{T}}^{\ell},\ p_{\mathrm{T}}^{\mathrm{miss}})$ fits
- Observed $p_{\mathrm{T}}^{\mathrm{W}}$ spectrum also sensitive to calorimeter response and resolution parameters

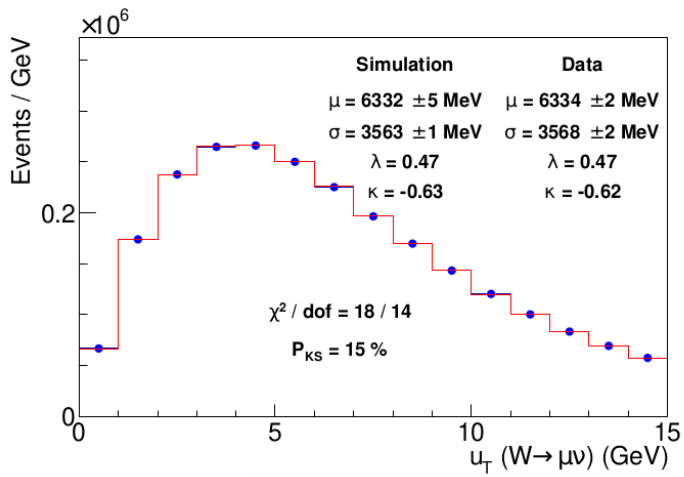

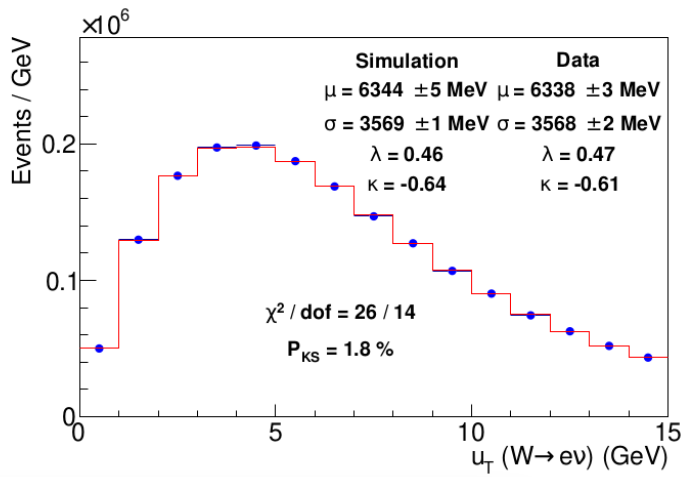

RESBOS Comparison

- arXiv:2205.02788 (J. Isaacson, Y. Fu, C-P. Yuan)
  - Compares NNLL+NLO RESBOS used in CDF measurement to N³LL+NNLO RESBOS2
  - Concludes < 10 MeV potential bias

	Mass Shift [MeV]	
Observable	ResBos2	+Detector Effect+FSR
m_T	1.5 ± 0.5	$0.2 \pm 1.8 \pm 1.0$
$p_T(\ell)$	3.1 ± 2.1	$4.3 \pm 2.7 \pm 1.3$
$p_T(\nu)$	4.5 ± 2.1	$3.0 \pm 3.4 \pm 2.2$

TABLE II. Summary of the shift in M_W due to higher order corrections. For reference, the CDF result was 80,433 ± 9 MeV [2] and the SM predicted value is 80,359.1 ± 5.2 MeV [1]. The second column shows the shift in the mass neglecting detector effects and final state radiation (FSR), while the third column includes an estimate for detector effects and FSR in the mass shift. The first uncertainty is the statistical uncertainty induced in the mass extraction due to the number of ResBos events generated for the pseudoexperiments and the mass templates. The second uncertainty is the detector effect uncertainty calculated by using 100 different smearings of the data to extract the W mass. Additional details on the smearing can be found in Appendix C.

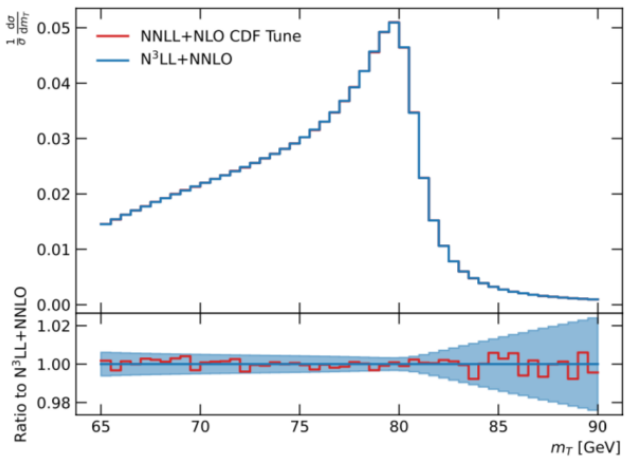

FIG. 4. W mass fit results to the pseudoexperiment for m_T. The pseudodata is generated at N³LL+NNLO accuracy with the default BLNY parametrization. The tuned NNLL+NLO results are then used for a template fit to extract the W mass [2]. The tuning resulted in a best fit value of $g_2 = 0.66$ GeV^{-2} and $\alpha_s(M_Z) = 0.120$. The best fit mass (80,386 MeV) is shown in red. The blue band represents the statistical uncertainty of the CDF result. Detector effects and FSR are not included here, but the corresponding result for m_T can be found in Appendix C.

Lepton Efficiency Measurements

- Very high selection efficiencies due to the loose set of requirements
- Efficiencies estimated in data using a tag-and-probe method
- Reduction in efficiency for large negative values of $u_{||}$ is due to an increase in overall hadronic activity in the event

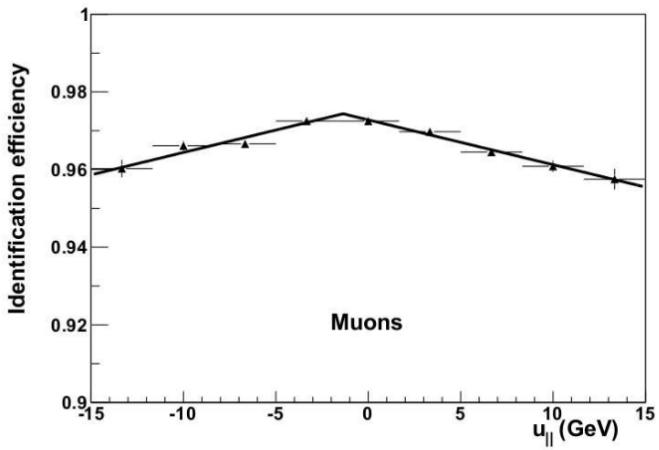

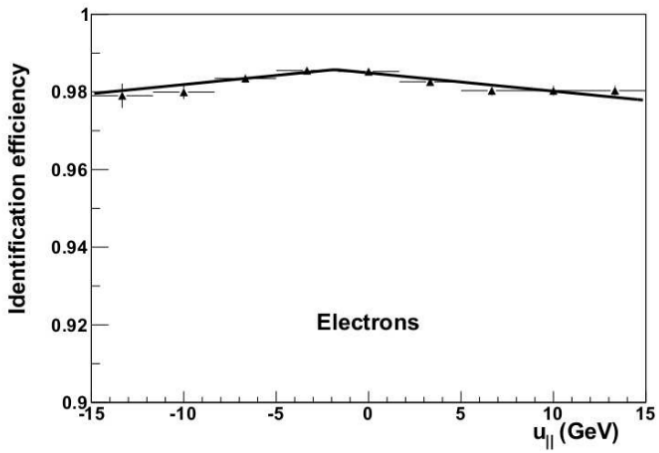

- The η-dependent efficiency for reconstructing leptons due to track trigger requirements is measured using W-boson events collected with a trigger with no track requirement
  - negligible impact in m_{W} measurement

Z Boson Event Selection & Background Estimation

- Single lepton triggers: loose lepton track and muon stub / calorimeter cluster requirements, with $p_{\mathrm{T}}^{\ell} > 18$ GeV
  - trigger efficiency ∼100%
- Offline lepton selection:
  - Electron cluster $E_{\mathrm{T}} > 30$ GeV, track $p_{\mathrm{T}} > 18$ GeV
  - Muon track $p_{\mathrm{T}} > 30$ GeV
  - Loose identification requirements
- $66 < m_{\ell\ell} < 116$ GeV
- $p_{\mathrm{T}}^{\ell\ell} < 30$ GeV
- $N(\mathrm{Z} \to \mu\mu/\mathrm{ee}) \sim 238/66$ K

Background Estimation in the W Boson Sample

- $\mathrm{Z} \to \ell\ell$ events with only one reconstructed lepton
  - efficiency and calorimeter response mapped using control samples of $\mathrm{Z} \to \ell\ell$ data, and modeled in the custom simulation
- $\mathrm{W} \to \tau\nu \to \ell\nu\nu$ background estimated using custom simulation
- QCD jet background estimated using control samples of data, anti-selected on lepton quality requirements
- Pion and kaon decays-in-flight to mis-reconstructed muons
  - estimated using control samples of data, anti-selected on muon track-quality requirements
- Cosmic ray muons estimated using a dedicated track-finding algorithm

Cosmic Muon Momentum Alignment

First step is the alignment of COT using cosmic muons

Two degrees of freedom (shift & rotation) for each of 2520 cells made up of twelve sense wires constrained using hit residuals from cosmic-ray tracks

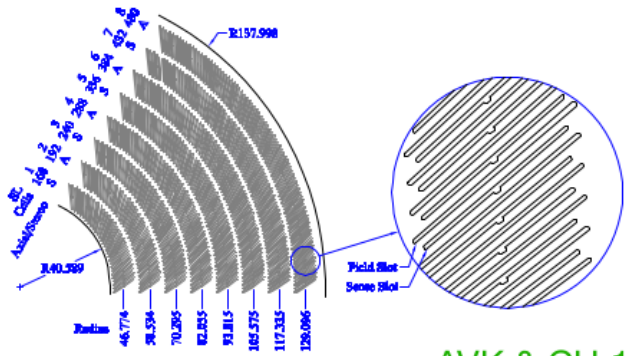

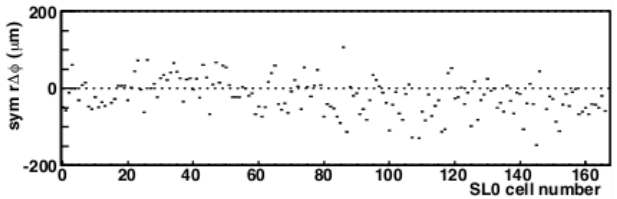

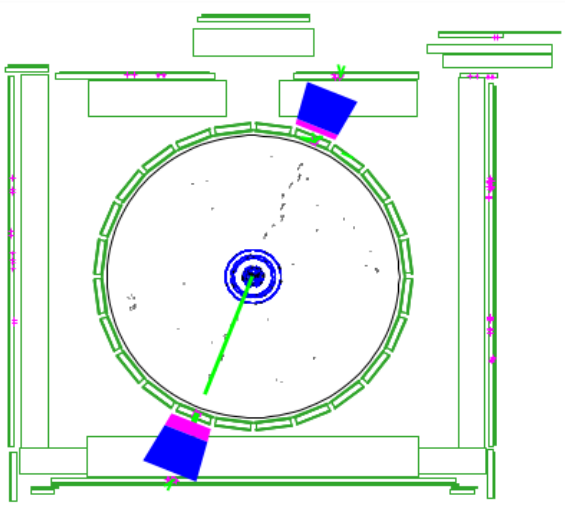

AVK & CH,1404.3457 & NIM A 762, 85 (2014)

Two parameters for the electrostatic deflection of the wire within the chamber constrained using difference between fit parameters of incoming and outgoing cosmic-ray tracks

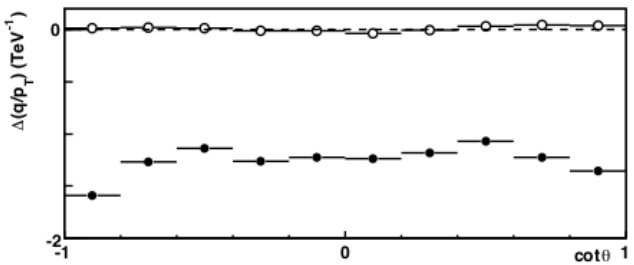

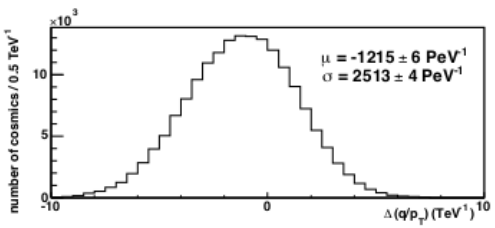

Before

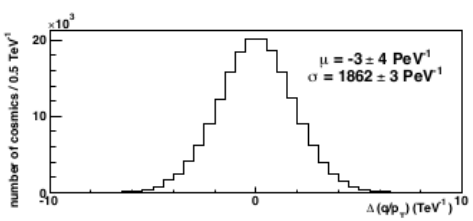

After

J/ψ & Upsilon Muon Momentum Calibration

Second step is the scale calibration from J/ψ decays to muons

Model lineshape using hit-level simulation and NLO form factor for QED radiation

Apply correct the length scale of the tracker with mass measurement as a function of $\Delta \cot \theta$

Correct the amount of upstream material with mass measurement as a function of p_T^{-1}

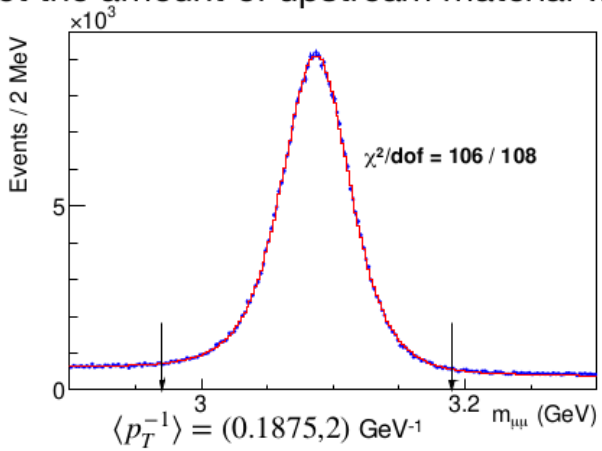

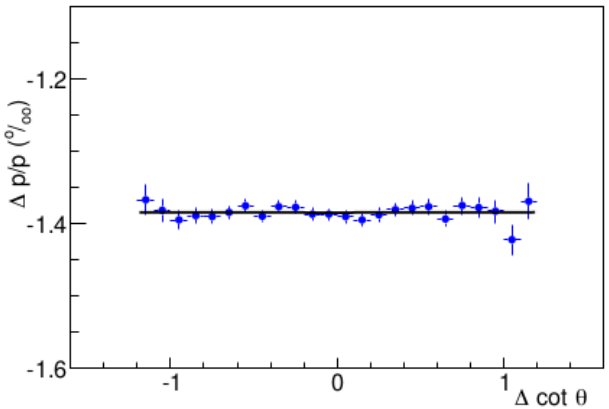

Third step is the scale calibration from Υ decays to muons

Compare fit results with and without constraining the track to the collision point

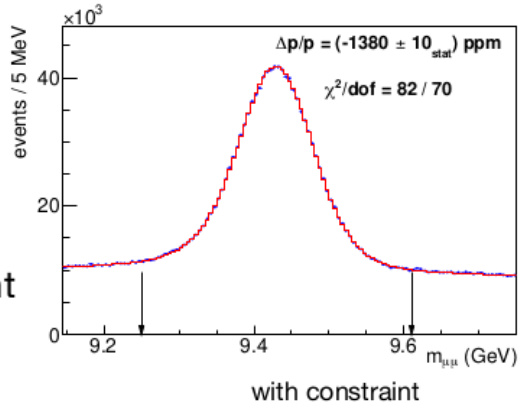

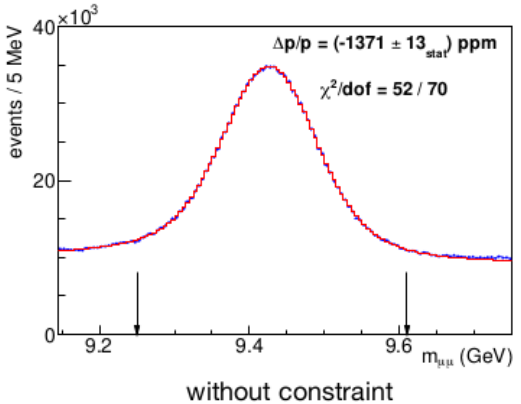

Recoil Model

- Parametrize recoil model using two components and tune using data
- Soft "spectator interaction" component
  - randomly oriented (~ 3 additional interactions per event)
  - modeled using minimum-bias data
- Hard "jet" component
  - boson p_{T} dependent response and resolution
  - tune by balancing boson p_{T} and recoil in Z events
- Recoil scale $R = u_{meas}/u_{true}$
  - $R = a log(b u_T^{true}/GeV)/log(15b)$
  - calibrate by balancing Z p_{T} against $p_{\mathrm{T}} + u$ along η axis
- Recoil energy resolution
  - calibrate balancing Z p_{T} against rms$(p_{\mathrm{T}} + u)$
  - dijet events contribute resolution term in ξ direction

Recoil Calibration Details (I)

First step is the alignment of the calorimeters

Misalignments relative to the beam axis cause a modulation in the recoil direction

Alignment performed separately for each run period using min bias data

Second step is the reconstruction of the recoil

Remove towers traversed by identified leptons

Remove corresponding recoil energy in simulation using towers rotated by 90°

validate using towers rotated by 180°

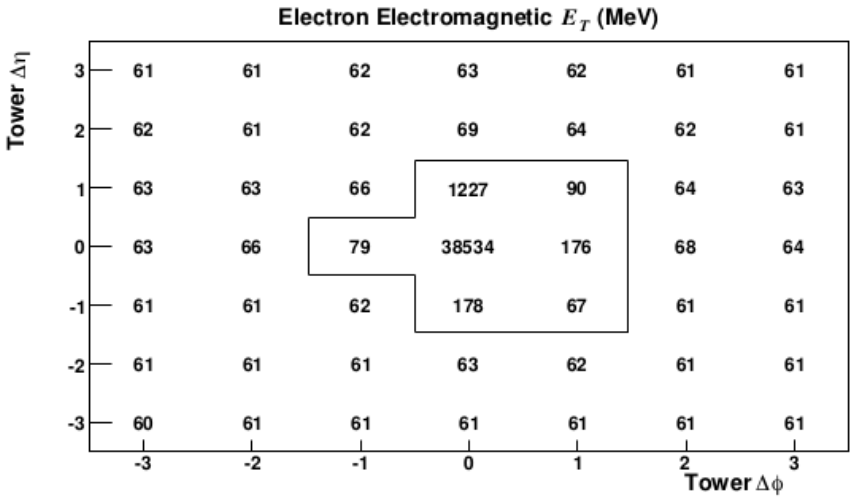

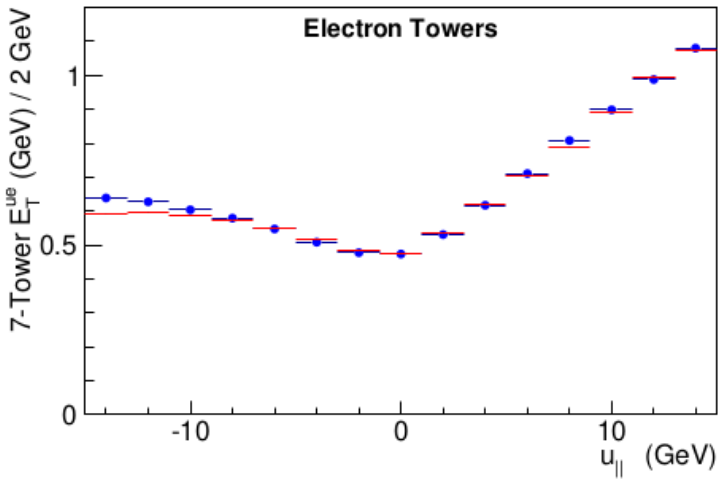

Recoil Calibration Details (II)

Third step is the calibration of the recoil response

Use ratio of recoil magnitude to p_T^Z along direction of p_T^Z

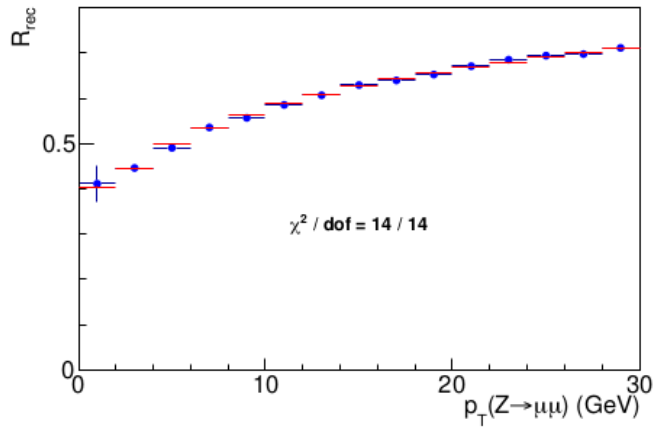

Fourth step is the calibration of the recoil resolution

Includes jet-like energy and angular resolution, additional dijet fraction term, and pileup

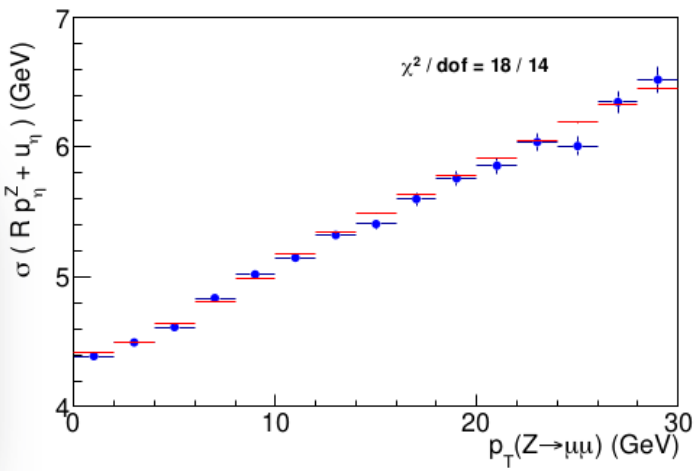

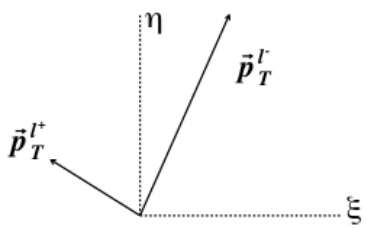

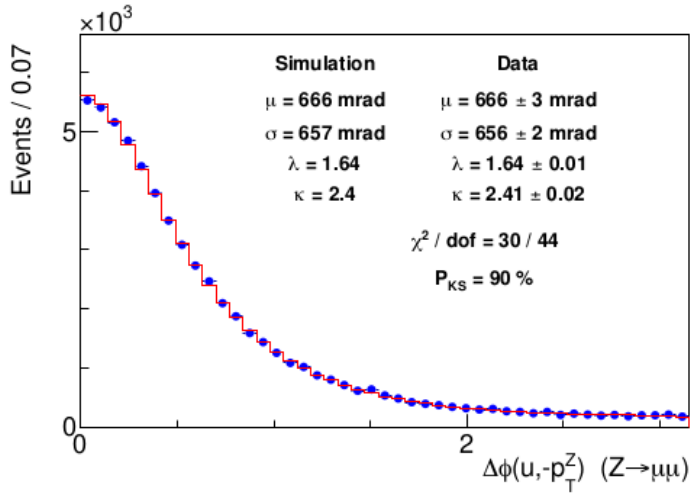

Recoil Modeling: Systematic Uncertainties

Parameter	Description	Source	m_T	p_T^ℓ	p_T^ν
a	average response	Fig. S23	−1.6	−2.9	−0.2
b	response non-linearity	Fig. S23	−0.8	−2.0	0.7
Response			1.8	3.5	0.7
N_V	spectator interactions	Fig. S24	0.5	−3.2	3.6
s_{had}	sampling resolution	Fig. S24	0.3	0.3	0.8
$f_{\pi^0}^4$	EM fluctuations at low u_T	Fig. S25	−0.3	−0.2	−1.0
$f_{\pi^0}^{15}$	EM fluctuations at high u_T	Fig. S25	−0.3	−0.3	−0.2
α	angular resolution at low u_T	Fig. S26	1.4	0.1	2.5
β	angular resolution at intermediate u_T	Fig. S26	0.2	0.1	0.7
γ	angular resolution at high u_T	Fig. S26	0.3	0.3	0.7
f_2^a	average dijet component	Fig. S27	0.1	−1.1	0.8
f_2^s	variation of dijet component with u_T	Fig. S27	−0.1	−0.2	−0.1
k_ξ	average dijet resolution	Fig. S28	−0.1	0.1	−0.3
δ_ξ	fluctuations in dijet resolution	Fig. S28	−0.2	0.2	−1.1
A_ξ	higher-order term in dijet resolution	Fig. S28	0.1	−1.0	0.7
μ_ξ	—"—	Fig. S28	−0.5	−0.4	−0.9
ϵ_ξ	—"—	Fig. S28	0.1	−0.2	0.4
S_ξ^+	—"—	Fig. S28	0.5	−0.4	1.4
S_ξ^-	—"—	Fig. S28	−0.3	−0.2	−0.5
q_ξ	—"—	Fig. S28	−0.2	0.0	0.2
Resolution			1.8	3.6	5.2

Recoil Modeling: Energy Response

The recoil response function is defined as the ratio of measured recoil to true recoil, projected along the direction of the true recoil $R \equiv \vec{u}_T \cdot \hat{u}_T^{\text{true}} / u_T^{\text{true}}$, where $\vec{u}_T^{\text{true}} = -\vec{p_T}^{W,Z}$ is the net $\vec{p}_T$ of the initial-state radiation. The function

$$R = a \log(b u_T^{\text{true}}/\text{GeV}) / \log(15b) \quad , \tag{S15}$$

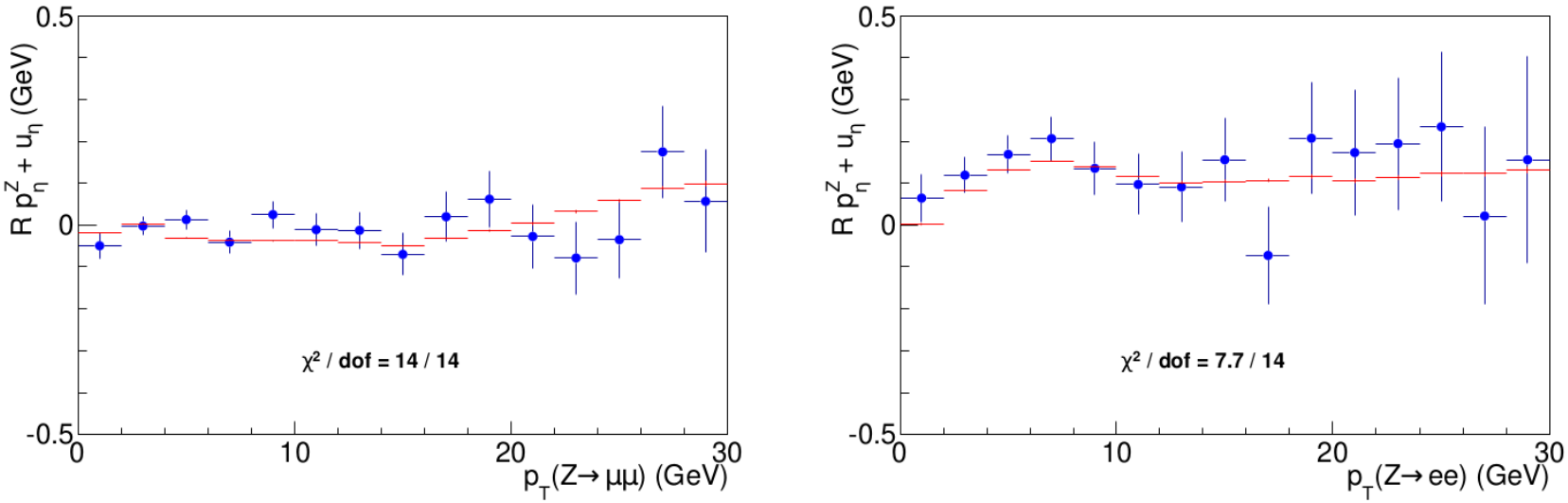

FIG. S23: Distribution of $Rp_\eta^{\ell\ell} + u_\eta$ for Z-boson decays to muons (left) and electrons (right) as a function of Z-boson p_T in simulated (lines) and experimental (circles) data. The detector response parameters a and b (Eq. S15) are obtained by minimizing the combined χ^2 of these distributions.

Recoil Modeling: Energy Resolution (I)

The resolution on the magnitude of the simulated recoil is parametrized with a sampling term, simulated with a Laplacian random variable with rms

$$\sigma(u_T) = s_{\text{had}}\sqrt{u_T^{\text{true}}/\ \text{GeV}}\ , \tag{S17}$$

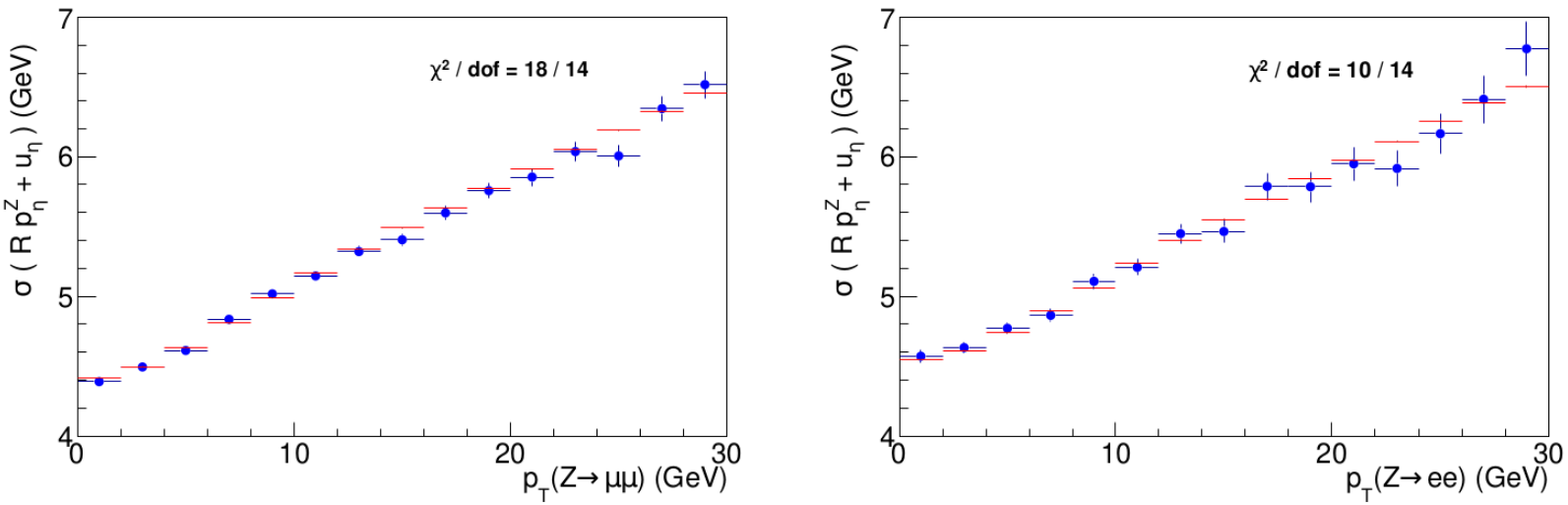

FIG. S24: Resolution on $Rp_\eta^{\ell\ell} + u_\eta$ in simulated (lines) and experimental (circles) data for Z-boson decays to muons (left) and electrons (right).

Recoil Modeling: Energy Resolution (II)

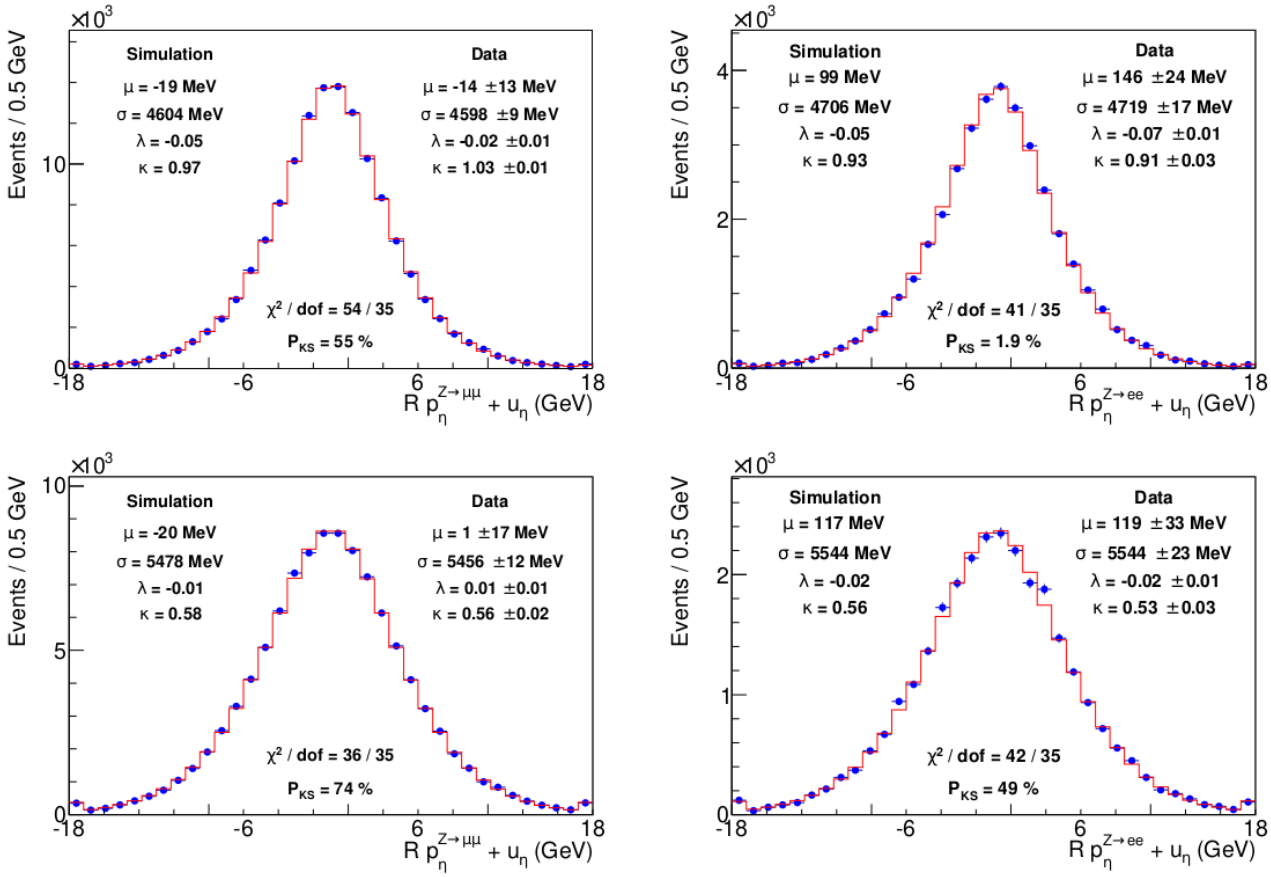

FIG. S25: Distributions of the p_η-balance for $p_T^{\ell\ell} < 8$ GeV (top) and $8 < p_T^{\ell\ell} < 30$ GeV (bottom), for the muon (left) and electron (right) channels. The first four moments [mean (μ), rms (σ), skewness (λ), and excess kurtosis (κ)] are shown.

- Skewness is a measure of the asymmetry of the probability distribution of a real-valued random variable about its mean
- Excess Kurtosis is a measure for a standard normal distribution of whether the data are heavy-tailed or light-tailed relative to a normal distribution

Recoil Modeling: Angular Resolution

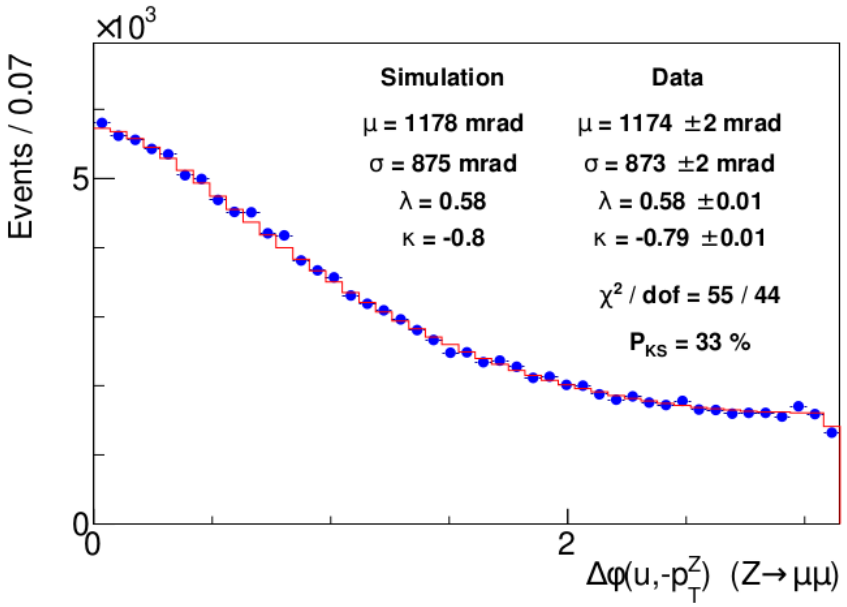

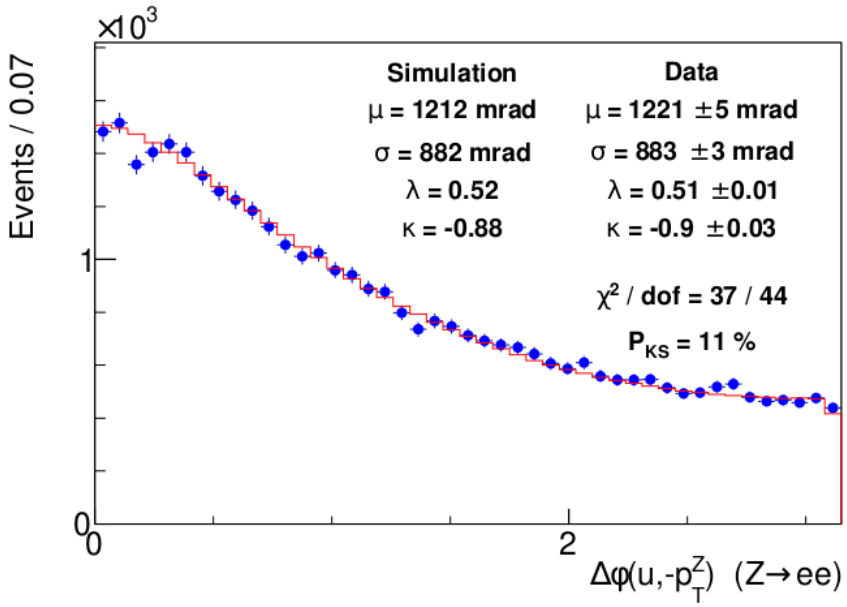

- Distributions of the difference in azimuthal angles of $\vec{u}$ and -$\vec{p}_{\mathrm{T}}^{\ell\ell}$, shown in absolute value for $p_{\mathrm{T}}^{\ell\ell} < 8$ GeV. Distributions are shown for $Z \to \mu\mu$ (left) $Z \to \mathrm{ee}$ (right). The data (blue circles) are compared to the tuned simulation (red histogram)

Recoil Modeling: Dijet Components

$$f_2 = f_2^a + f_2^s u_T,\ f_2^a = (0.80 \pm 0.04_{\text{stat.}})\%,\ f_2^s = (44 \pm 6_{\text{stat.}})\%$$

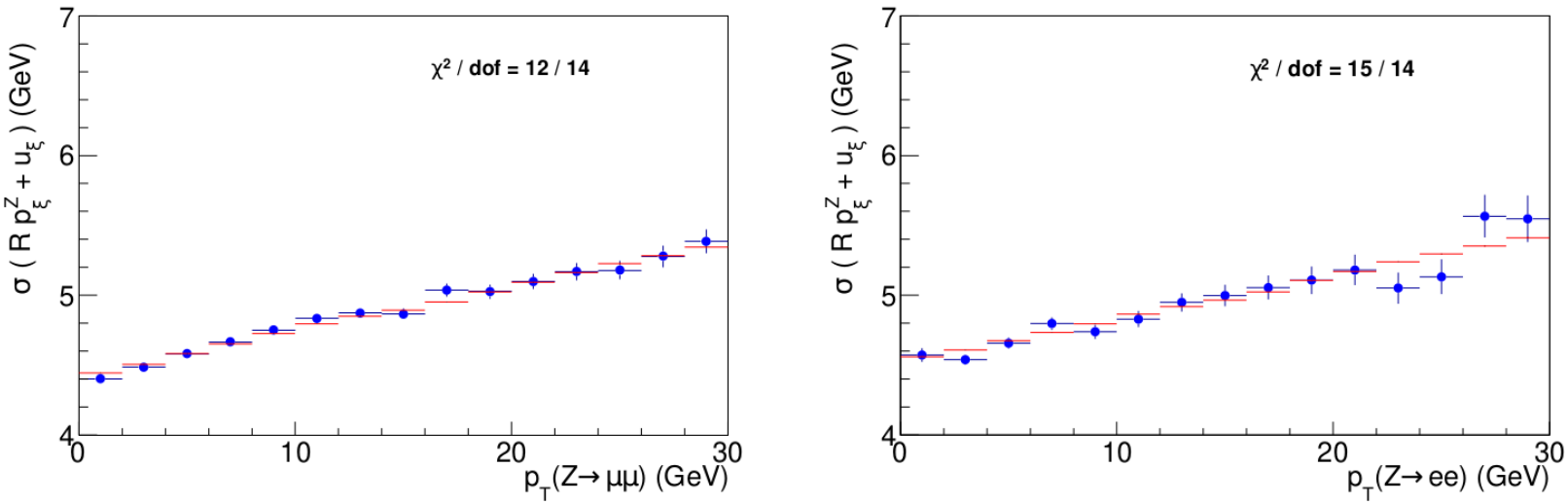

FIG. S27: Root-mean-square dispersion of the scaled p_T-balance in $Z \to \ell\ell$ data, projected onto the ξ axis, as a function of $p_T^{\ell\ell}$. The data (blue circles) for the muon (left) and electron (right) channels are compared to the tuned simulation (red histogram). These plots are used to tune the dijet resolution parameters f_2^a and f_2^s, whose values are given in Eq. (S22).

Recoil Modeling: Dijet Resolution

The recoil resolution function due to the dijet component is modeled with a Gaussian distribution with mean k_ξ and rms= $k_\xi \delta_\xi$, symmetrized in the ξ-direction. The parameters k_ξ and δ_ξ are tuned on the one-dimensional distributions of the p_ξ-balance in the sub-samples $p_T^{\ell\ell} < 8$ GeV and $8 < p_T^{\ell\ell} < 30$ GeV (see Fig. S28). The fitted parameter values are

$$k_\xi = (10.0 \pm 0.2_{\rm stat})\ {\rm GeV} \quad , \quad \delta_\xi = (27.5 \pm 3.0_{\rm stat})\% \quad . \tag{S23}$$

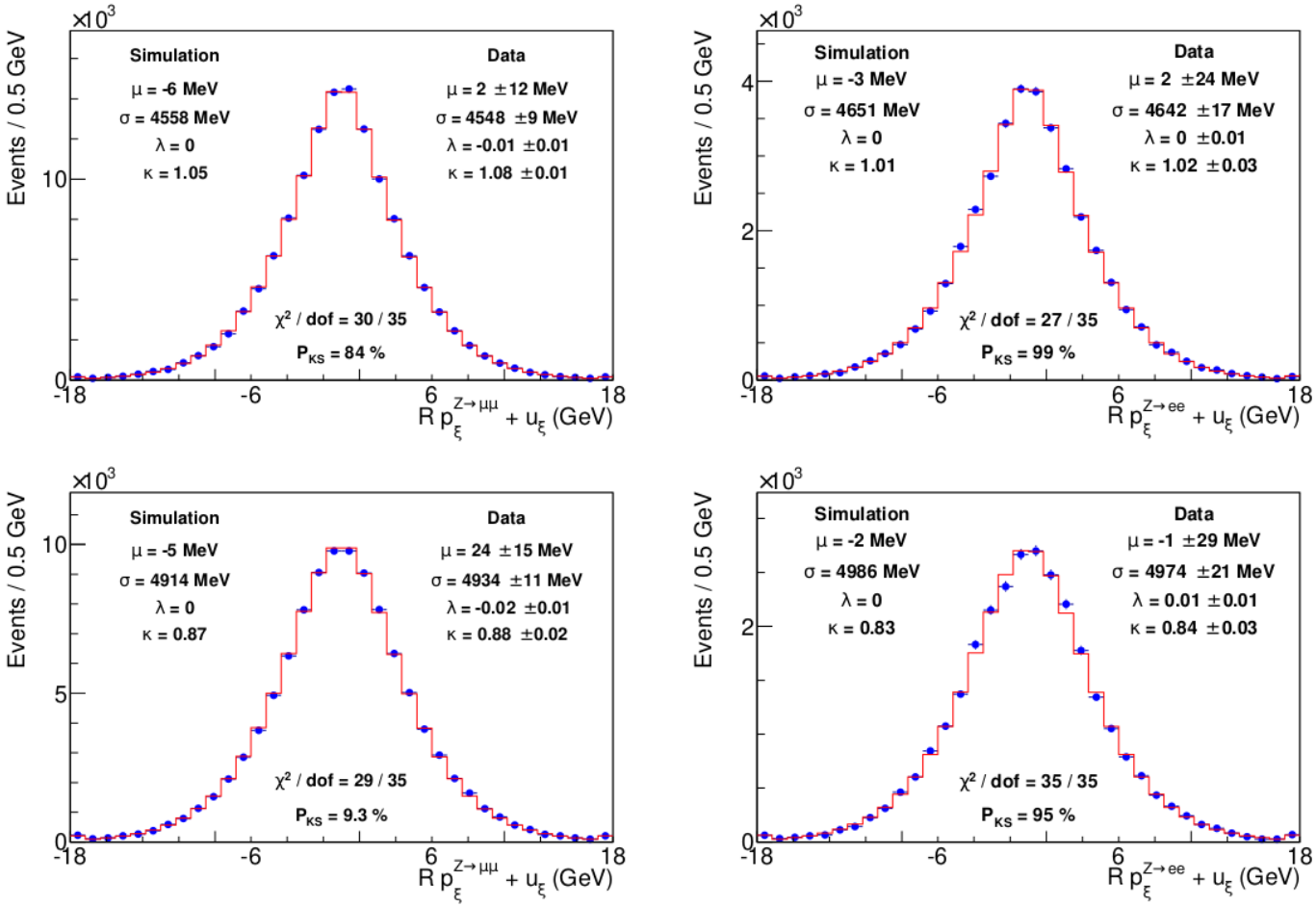

FIG. S28: Distributions of the p_ξ-balance for $p_T^{\ell\ell} < 8$ GeV (top) and $8 < p_T^{\ell\ell} < 30$ GeV (bottom), for the muon (left) and electron (right) channels. The first four moments, mean (μ), rms (σ), skewness (λ), and excess kurtosis (κ) are shown. The data (blue circles) are compared to the tuned simulation (red histogram). These plots are used to tune the dijet resolution parameters k_ξ and δ_ξ, whose values are given in Eq. (S23), as well as A_ξ, μ_ξ, ϵ_ξ, $S_\xi^\pm$ and q_ξ,

Analysis Changes since 2012 (I)

- Use of a single "constant term" for the calorimeter resolution is improved in this analysis by making the constant term a linear function of the absolute value of pseudorapidity
  - measured width of the $\mathrm{Z} \rightarrow \mathrm{ee}$ peak is found to be consistent with this resolution mode
- Uniformity of the COT calibration is significantly enhanced by an alignment of the COT wire-positions using cosmic-ray data
  - residual biases that were not resolved in the previous iteration of the alignment were eliminated in this iteration
- Temporal uniformity calibration of the EM calorimeter is introduced in this analysis. The calorimeter response in each longitudinal tower is studied as functions of experiment operational time, and the time-dependence is corrected for
  - in the previous analysis the time dependence of the response was not studied or corrected for, beyond the standard uniformity calibration

Analysis Changes since 2012 (II)

- Procedure of tuning the recoil angular smearing model on the distributions of the azimuthal angle difference between the recoil vector and the dilepton p_{T} vector in $\mathrm{Z} \to \ell\ell$ data is a new feature of the analysis
- Procedure of tuning the kurtosis of the recoil energy resolution on the distributions of p_{T}-balance in the $\mathrm{Z} \to \ell\ell$ data is a new feature of the analysis
- Better model the energy resolution fluctuations arising from multiple interactions
- Fluctuations in the energy flow from spectator parton interactions and additional proton-antiproton collisions contribute to the recoil resolution. These fluctuations are measured from zero-bias data

Analysis Changes since 2012 (III)

- New procedure for matching the luminosity profiles, separately for each channel
  - confirmed by comparing the data and simulated distributions of $\sum E_T$ for the W and Z boson data in each channel
- Use of a theoretical calculation of the $p_{\mathrm{T}}^{\mathrm{W}}/p_{\mathrm{T}}^{\mathrm{Z}}$ spectrum ratio to study its QCD scale variation is a new feature of this analysis
- Constraint from the $p_{\mathrm{T}}^{\mathrm{W}}$ data spectrum is another new feature that incorporates additional information compared to the previous analysis
  - in the past, only the $p_{\mathrm{T}}^{\mathrm{Z}}$ data spectrum was used to constrain the production model

Systematic uncertainty from 15 MeV to 6.9 MeV (I)

- Lepton and recoil energy scale and resolution uncertainties are data-driven and expected to scale by statistics
  - recoil response and resolution model now extracts more information from the data than previous analysis
- Uncertainties due to lepton efficiency and lepton removal are data-driven
  - improvement in the modeling of the EM calorimeter resolution eliminated an additional source of uncertainty in the previous analysis
- Uncertainties due to backgrounds, though data-driven, contain contributions obtained from comparing different methods of background determination
  - not expected to have reduced uncertainties

Systematic uncertainty from 15 MeV to 6.9 MeV (II)

- Systematic uncertainty due to PDFs is reduced by switching from the CTEQ6 set to the much newer NNPDF3.1 set and using the mathematically well-defined "replica" method of obtaining uncertainties from the latter set
- Constraint on the boson p_{T} spectrum from the $p_{\mathrm{T}}^{\mathrm{Z}}$ data are expected to scale with the available sample
  - additional constraint from the $p_{\mathrm{T}}^{\mathrm{W}}$ data wa not applied in the previous analysis and further reduces the uncertainty

Dimuon Mass

CDF

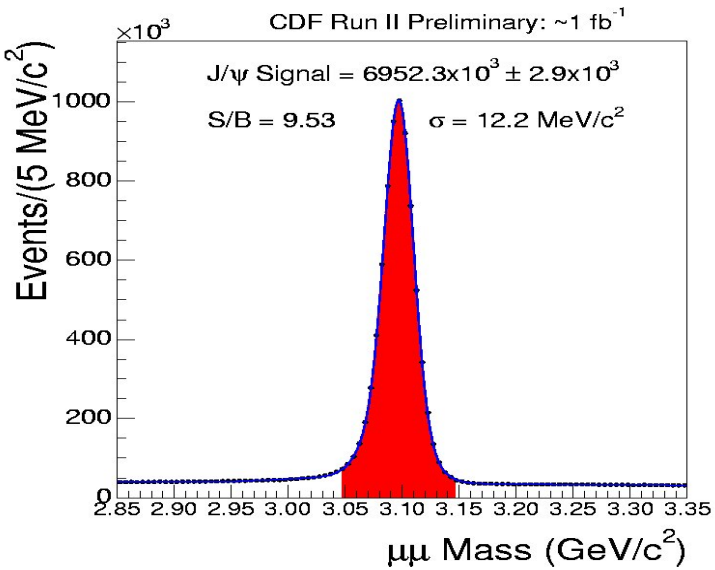

LHCb

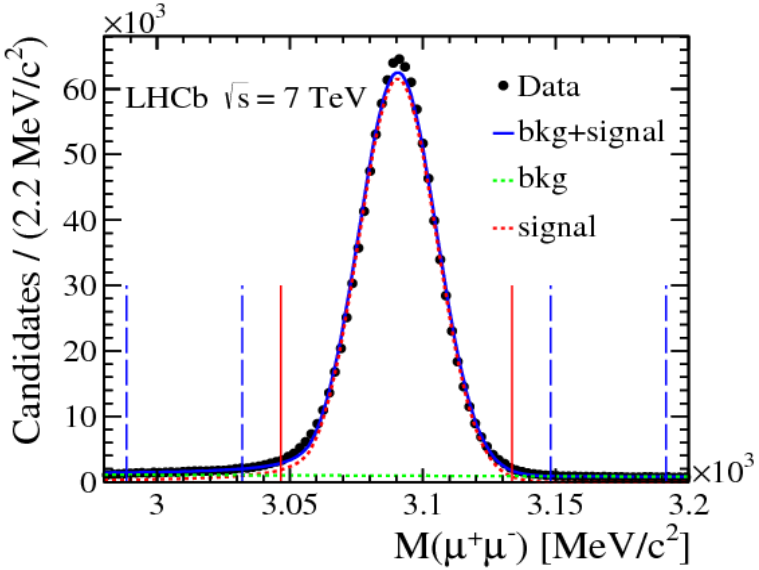

CMS

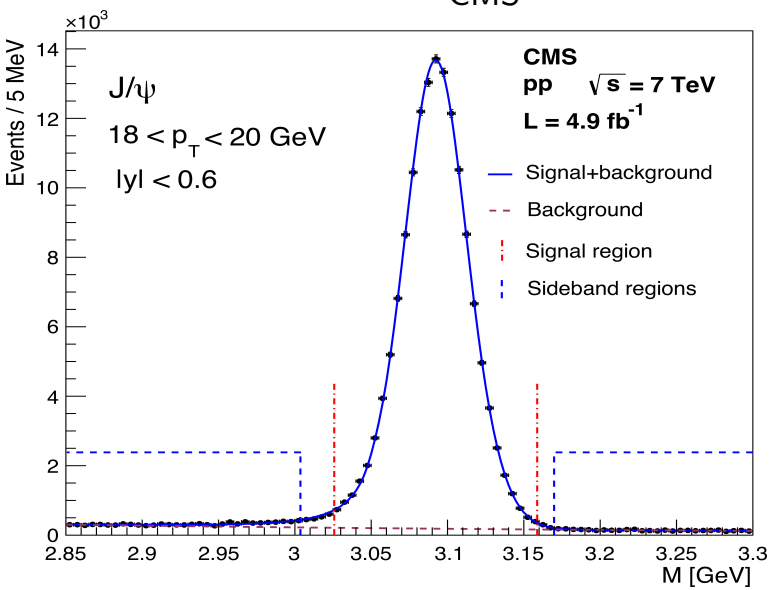

ATLAS

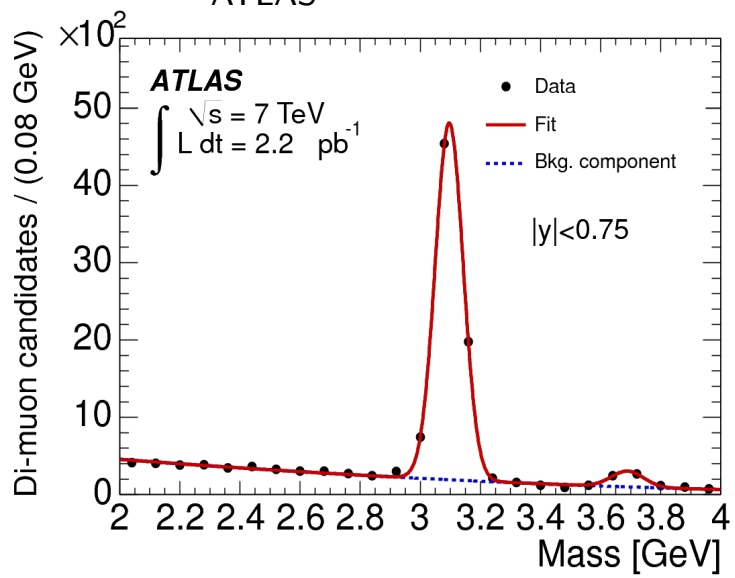

m_T Fits

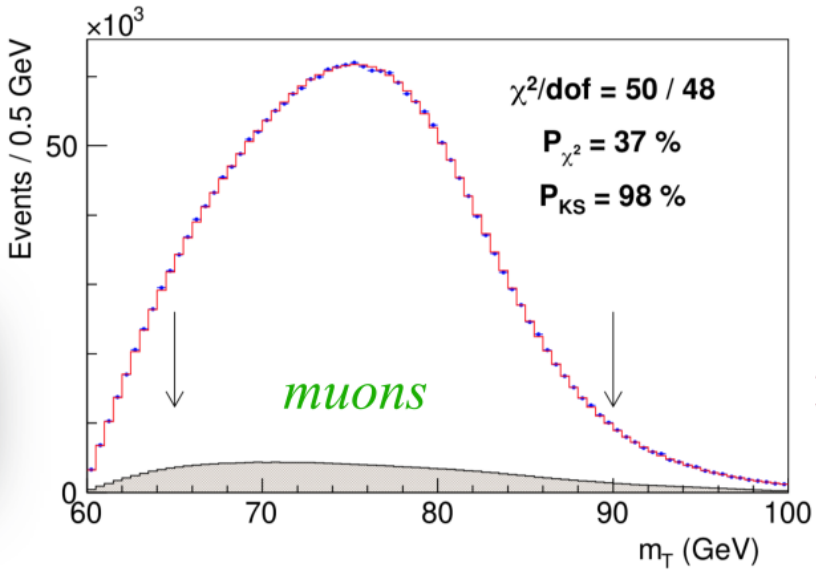

Fig. 4

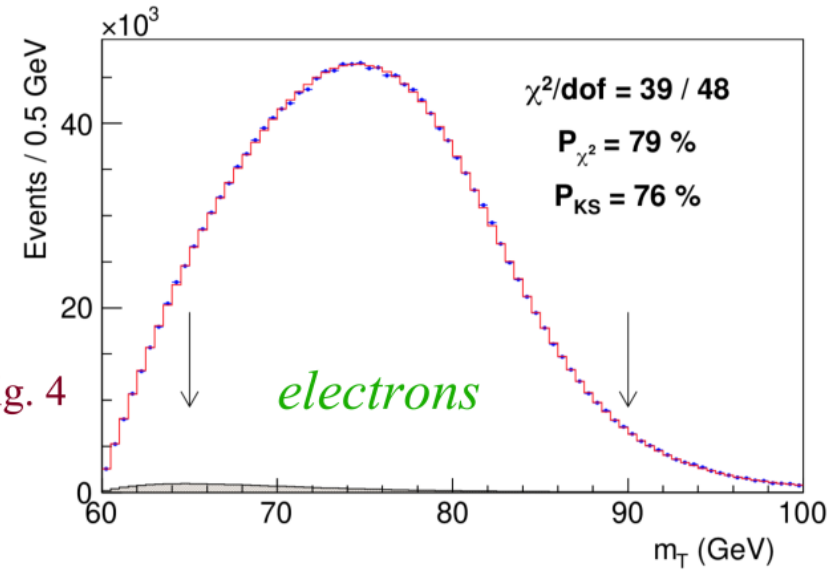

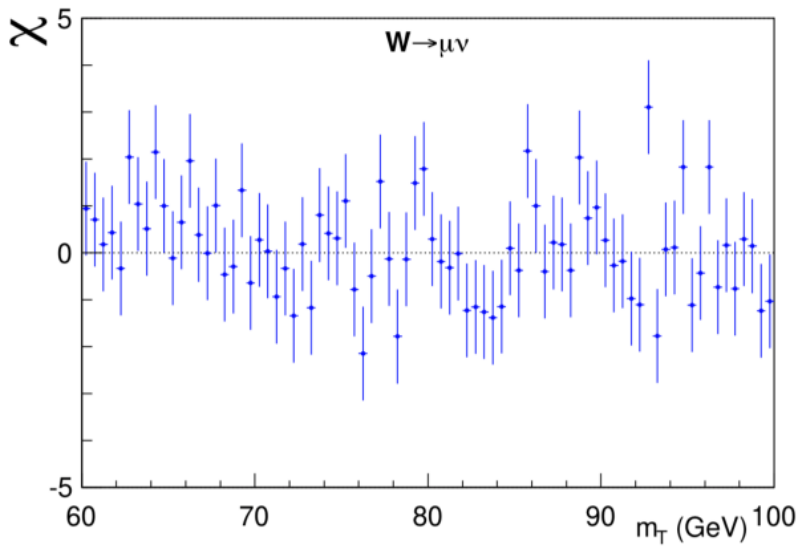

Fig. 36

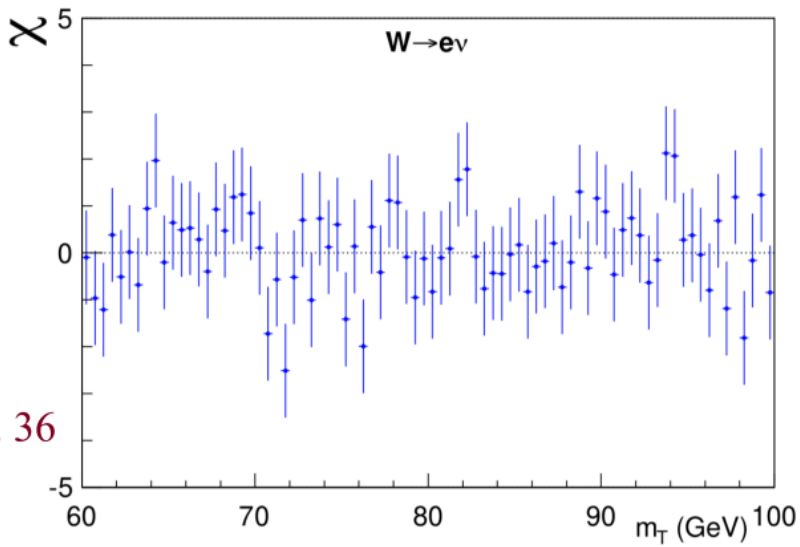

p_{T}^{ℓ} Fits

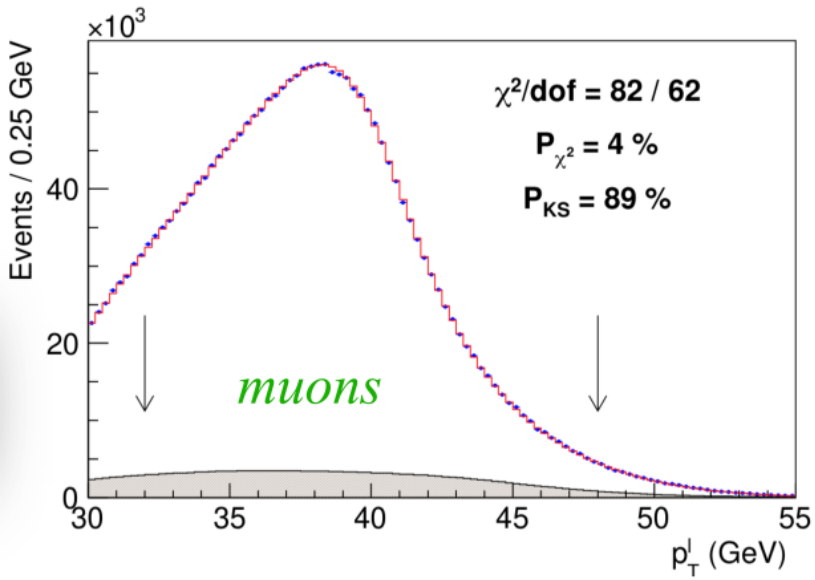

Fig. 4

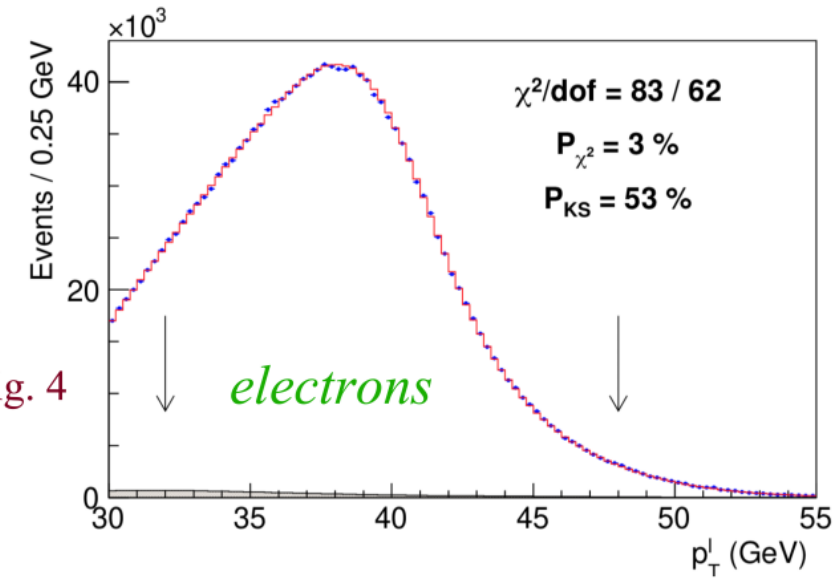

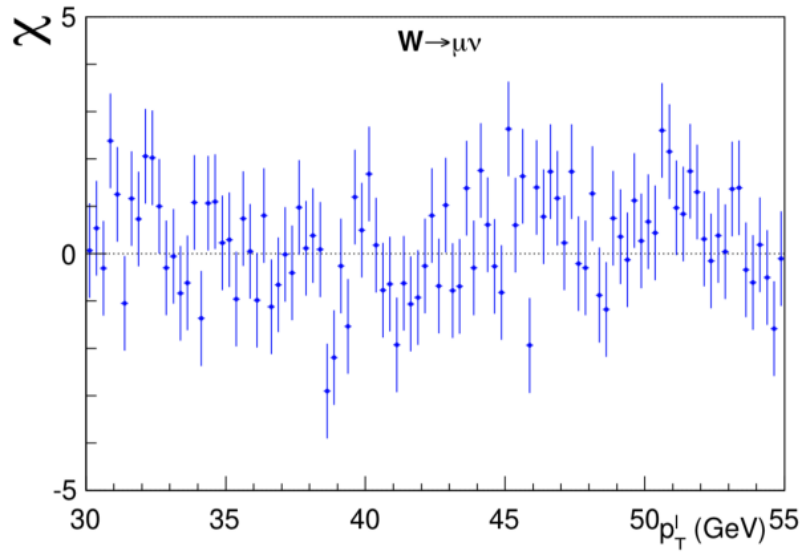

Fig. 37

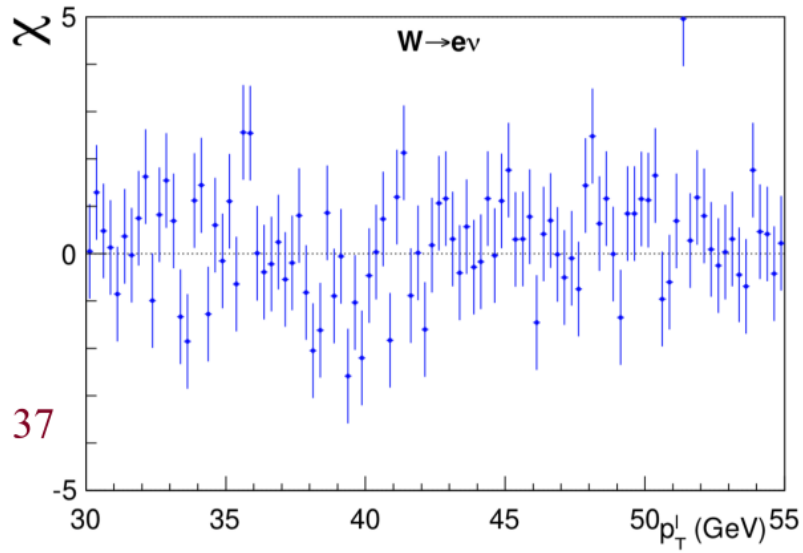

p_T^{miss} Fits

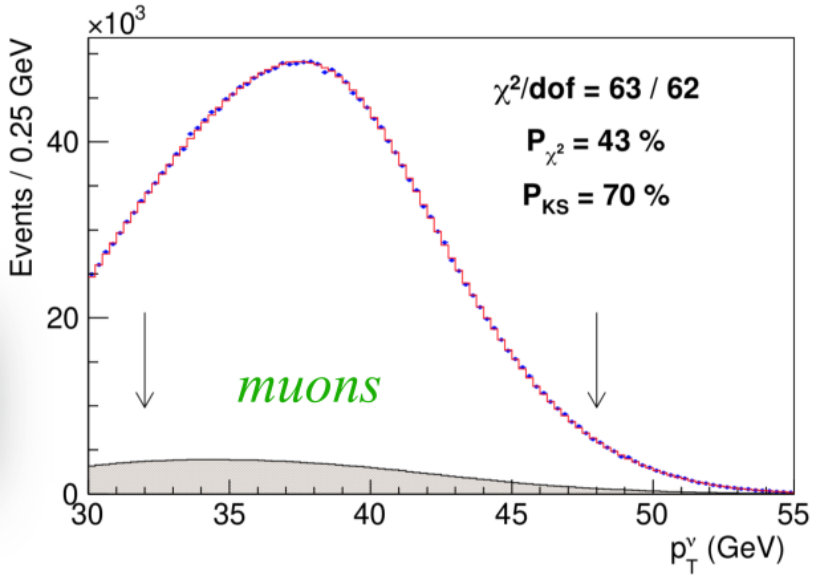

Fig. 4

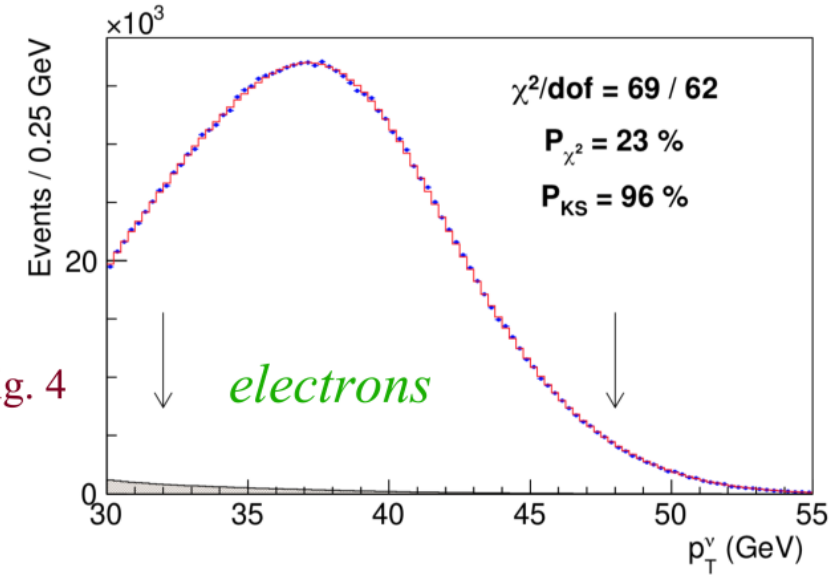

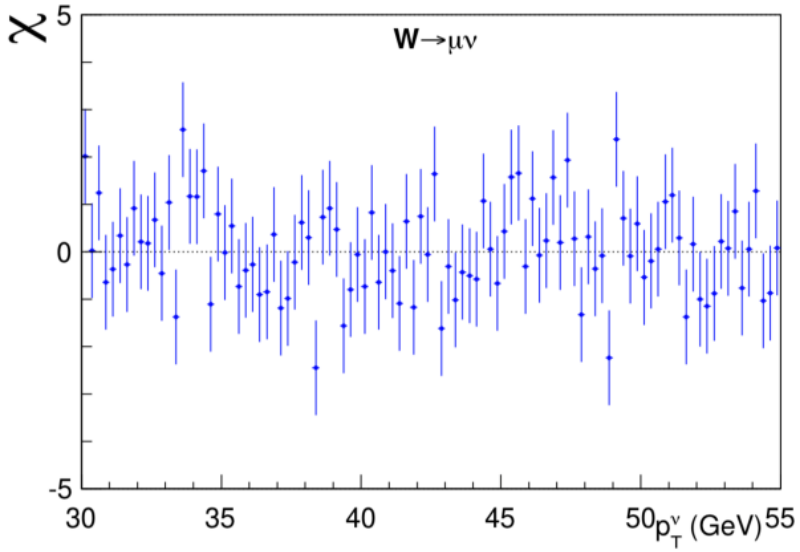

Fig. 38

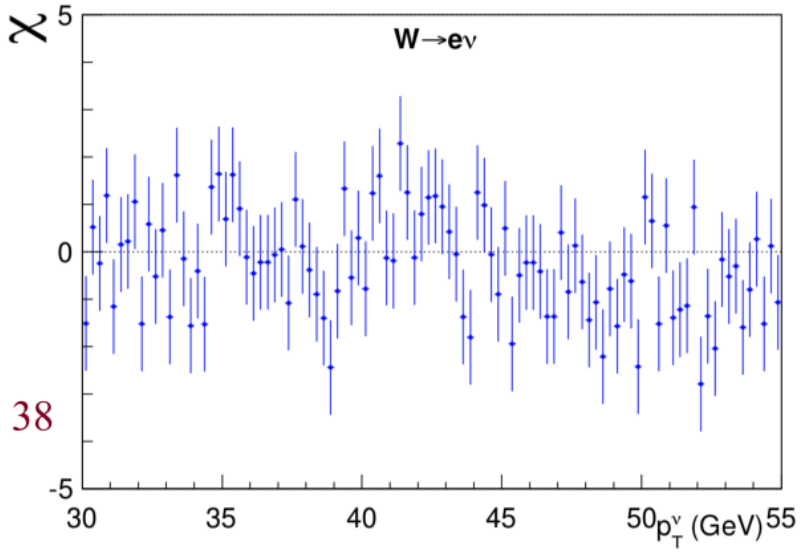

New Physics Explanations (with Link to Arxiv)

- Explanation of the W mass shift at CDF II in the Georgi-Machacek Model
- W-boson mass and electric dipole moments from colour-octet scalars
- Implications of W-boson mass for atomic parity violation
- CDF-II W Boson Mass Anomaly in the Canonical Scotogenic Neutrino-Dark Matter Model
- W-boson mass in the triplet seesaw model
- Dark photon kinetic mixing effects for CDF W mass excess
- Singlet-Doublet Fermion Origin of Dark Matter, Neutrino Mass and W-Mass Anomaly
- Extra boson mix with Z boson explaining the mass of W boson
- Interpreting the W mass anomaly in the vectorlike quark models
- W boson mass in Singlet-Triplet Scotogenic dark matter model
- CDF W mass anomaly in a Stueckelberg extended standard model
- W-Boson Mass Anomaly from Scale Invariant 2HDM
- Beta-decay implications for the W-boson mass anomaly
- W boson mass shift and muon magnetic moment in the Zee model
- On the W-mass and New Higgs Bosons
- ... And a very long et cetera

W-Like Mass Fit Using $Z \to \ell\ell$ Events?

- Was not considered worth pursuing given the relatively small data sample
  - $\sim$300K $Z \to \ell\ell$ events
- Example CMS analysis: CMS-PAS-SMP-14-007
  - using $\sim$200K $Z \to \mu\mu$ events, m_T fit only
  - $m_Z^{W-like} = 91206 \pm 36(\text{stat.}) \pm 30(\text{syst.})$ MeV
- Example ATLAS analysis: STDM-2014-18
  - using $\sim$1.8M $Z \to \ell\ell$ events, combining p_T^ℓ and m_T fits
  - $m_Z^{W-like} = 91159 \pm 16(\text{stat.}) \pm 12(\text{syst.})$ MeV
- Expected statistical uncertainty should be in between both analyses
  - a $\sim$ 25 MeV statistical uncertainty, i.e., about four times larger values than the actual W boson measurement was not considered interesting